

Kharazmi University Physics Department

A Thesis Submitted in Partial Fulfillment for the Degree of MS in Theoretical Physics

## Study Critical Phenomena via Holographic Approach

Ali Hosseinzadeh

Supervisor: Dr.Ali Vahedi

September 2022

## Abstract

In this thesis, we study some fundamental notions associated with black holes due to examine the holographic principle. By stating the holographic principle in the anti-de sitter space we quickly review anti-de sitter/conformal field theory correspondence (AdS/ CFT). We underline a holographic model due to the computing DC conductivity. Then, by using AdS/CFT correspondence we study a non-equilibrium phase transition in the presence of a constant external electric (magnetic field). Also, Using AdS/CFT correspondence, the phase transition in a system with a chiral magnetic effect is studied. We are going to explore the non-equilibrium critical behavior of the chiral magnetic effect by a holographic probe branes model, i.e. the spinning branes in the presence of an external magnetic field. We will find that this configuration has a phase transition structure when the chiral chemical potential changes.

## Dedication

Dedicated to the best teacher, I ever had but never seen!

## Leonard Susskind



## Declaration

This...

## Acknowledgement

I want to give thanks to my dear friends who have encouraged me to study physics, especially Dr.G.Azizpuri.Agd, F.Hossenifar, A.Ahmadpana, and A.Hosseinzadeh.

I would like to express my gratitude to my supervisor Dr.A.Vahedi.

I wish to extend my special thanks to my dear family for their support, especially dear Erfan.

I do not have any words to express my deep gratitude toward Dr.B.Shakerin for the useful discussions during my master thesis, and for everything he taught me.

## List of Figures

2.1	Graph of information	11
2.2	Conservation of phase space	13
2.3	Volume of the phase space and a sub-region	14
2.4	Event horizon	18
2.5	Event horizon	19
2.6	Hyperbolic coordinate	21
2.7	Hyperbolic coordinate and the horizon	22
2.8	Conflict between observers near the horizon	23
2.9	Near horizon proper distance	24
2.10	Cigar of the near horizon	26
2.11	Kruskal-Szekeres coordinate	28
2.12	Light cone coordinate	29
2.13	Compacted spacetime between $Y^+$ and $Y^-$ , more detail	30
2.14	Compacted spacetime between $Y^+$ and $Y^-$	31
2.15	Extended Penrose diagram for Schwarzschild black hole.	31
2.16	Shell of radiation, in the Penrose diagram	32
2.17	Shell of radiation, in the whole of Penrose diagram	33
2.18	The geometry of a black hole that is formed by an in-	
	falling shell	33
2.19	Heated string	36
	Breaking a string	37
2.21	Depict the excited string as a closed random walk on a	
	lattice in the plane	37
2.22	Create a black hole by Varying $g$	38
	The black hole/string transition	40
	Maximum entropy of a region of space	42
3.1	The AdS/CFT duality spans all physics arXivs!	43
3.2	Quantum phases	46
3.3	strange metal	47
4.1	$m_{a}$ - $J$ curve	56

4.2	B- $J$ curve													58
4.3	$J$ - $\omega$ curve													59

 $LIST\ OF\ FIGURES$ 

LIST OF FIGURES

## List of Tables

<i>1</i> 1	D3 = 1	7	embedding.										5	2
4.1	D3-1	ノし	embedding.										$^{\circ}$	J

## Contents

1	Intr	oducti	on	10
2	Put	Black	hole and Entropy toward Holographic prin-	
	$\operatorname{cipl}$	e		11
	2.1	Conser	rvation of Information	11
		2.1.1	Minus first law of physics!	11
		2.1.2	Entropy and statistical mechanics	12
		2.1.3	Entropy or temperature, which one is more fun-	
			damental?	12
		2.1.4	Liouville's theorem	12
		2.1.5	Poincaré recurrence theorem	13
		2.1.6	A little bit! information theory	14
	2.2	Black	Holes	17
		2.2.1	Simplest black hole	17
		2.2.2	The nature of horizon	18
		2.2.3	The conflict between Alice and Bob is near the	
			horizon!	20
		2.2.4	Some useful coordinate systems	23
		2.2.5	Carter–Penrose diagrams	28
		2.2.6	Formation of black holes	32
	2.3	Hologr	aphy and Black Holes Thermodynamics	34
		2.3.1	Entropy of a black hole	34
		2.3.2	Luminosity of the black holes	35
		2.3.3	Sting theory and black holes	35
		2.3.4	Holographic principle	40
3	AdS	S/CFT	and Critical Phenomena	43
	3.1	AdS/C	CFT Correspondence	43
		3.1.1	A qualitative description of AdS/CFT	43
		3.1.2	AdS space	44
		3.1.3	Holography in AdS space	45

CONTENTS

	3.2	Ads/C	CFT and Critical phenomena	46
		3.2.1	Quantum phases	46
		3.2.2	Holographic DC conductivities from the open	
			string metric	47
		3.2.3	the real-action method	48
4	The	Real-	Action Method, Chiral Magnetic Effect, and	
	We	yl Sem	imetal	49
	4.1	Karch	-O'Bannon's real-action method	49
		4.1.1	Metallic AdS/CFT	49
		4.1.2	The prob brane and conductivity	50
	4.2	Negat	ive Differential Resistivity	52
	4.3	Chiral	Magnetic Effect	52
		4.3.1	Reviewing of Chiral Magnetic effect from Probe	
			branes holography	52
		4.3.2	Results and discussion	57
	4.4	Nega	tive Differential Resistivity of a Weyl Semimetal	
		from A	AdS/CFT	58
$\mathbf{A}$	Ger	neral r	elativity	60
$\mathbf{A}$	Stri	ngs an	nd D-branes	61

## Chapter 1

## Introduction

The holographic principle is one of the astonishing and practical tents of string theory which has several advantages to studying some fundamental aspects of some theories. A good example of this is studying critical phenomena via a holographic approach. The physics of critical phenomena plays a crucial role in describing the phase transition of phenomena like conductivity or superconductivity, especially by critical exponents. We utilize the holographic principle to study the phase transition of the electric and magnetic field from probe brane holography.

In the recent decade, AdS/CFT correspondence is developed in different areas of theoretical physics. Even condensed matter physicists use AdS/CFT to study and find a solution for some complected quantum phase or specific matter like strange metal.

The aim of this research is to take advantage of the anti-de Sitter / conformal field theory (AdS/CFT) correspondence as a holographic approach to study the non-equilibrium steady-state phase transition from probe brane holography.

The thesis is organized as follows:

Chapter 1 is the introduction and motivation.

In chapter 2, I will review the notion of entropy, black holes, and the Holographic principle.

In chapter 3, I will review AdS/CFT correspondence and some of the properties of metal, insulators, and superconductors.

In chapter 4, by a holographic approach compute the conductivity and study phase transition.

## Chapter 2

# Put Black hole and Entropy toward Holographic principle

#### 2.1 Conservation of Information

#### 2.1.1 Minus first law of physics!

The majority of physicists believe in the conservation of information[1]. We call it as "minus first law of physics," because without conservation of information, the equations of physics are meaningless. Figure 2.1 is an example of two simple systems to represent the conservation of information and the violation of that.

The amount of information that it takes to describe a system is constant in time, and the distinction between systems never disappears. Actually in practice information does disappear but not in principle. In other words, every system can be manipulated in such a way that the information is conserved and traceable. Also, there are some limitations that create the notion of inaccessible or hidden information.

In the next section we going are to quantify the notion of information in the context of statistical physics and quantum mechanics.

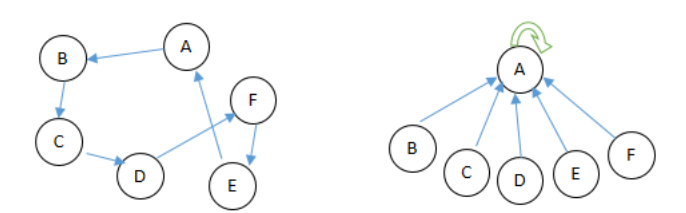


Figure 2.1: If reduce the information of the system to the label of the previous edge or next edge by a vertex, on the left every edge has complete information about the system. But on the right, the information is lost. For instance the stage of A you do not know what the previous edge was (note that on the right-hand A is a self-loop).

 $<sup>^1</sup>$ As coined by Leonard Susskind in his lecture below:https://theoreticalminimum.com/courses/cosmology-and-black-holes/2011/winter

#### 2.1.2 Entropy and statistical mechanics

The second law of thermodynamics can be stated in various ways [2], one of them is: "entropy always increases or stays the same." Based on some empirical facts, Joules per Kelvin was Carnot unit of entropy,

$$S_{carnot} = \Delta E/T, \tag{2.1}$$

where  $\Delta E$  is change in the energy and T is temperature. But in modern physics, we think of entropy as being measured in bits. A fundamental unit of entropy is the logarithm of 2 and that is dimensionless. Thus the entropy is hidden bits of information which is,

$$S_{statistical} = -\sum_{i=1}^{n} p_i \log_2 p_i, \tag{2.2}$$

where  $p_i$  is the probability that the system is in the *i*th state. Boltzmann constant plays a vital role to connect the microscopic and macroscopic worlds in physics, and we can find  $S_{carnot}$  in the context of statistical physics,

$$S = S_{carnot} = -k_B S_{statistical} = -k_B \sum_{i=1}^{n} p_i \log_2 p_i, \qquad (2.3)$$

where  $k_B$  is,  $1.380649 \times 10^{23} \ J.K^{-1}$ .

#### 2.1.3 Entropy or temperature, which one is more fundamental?

The temperature is defined based on entropy and vice versa. Actually, any attempt to define them independently is like the expression "cart before the horse". It is convenient for our purpose to define temperature based on entropy. Temperature is the change in entropy of the system if we add one bit of information to it (and vice versa to define entropy). Thus for one bit of information,

$$dE = T. (2.4)$$

#### 2.1.4 Liouville's theorem

Liouville's theorem states that volume in phase space is conserved over the evolution of a uniform probability distribution, i.e., the number of states is conserved. Figure 2.2 illustrates that the label (X, P) of every point changes but the volume is conserved.

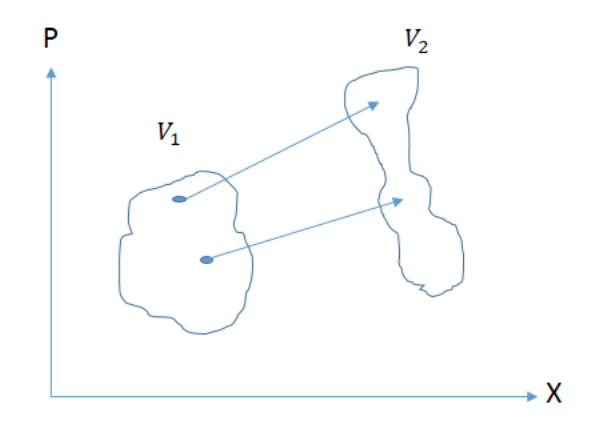


Figure 2.2:  $v_1$  and  $v_2$  are volumes of phase space which are the same

#### 2.1.5 Poincaré recurrence theorem

#### Classical version

The classical version<sup>2</sup> of the Poincaré recurrence theorem states that the evolution of trajectory of an isolated and finite system which is labeled by (p,q) in the phase space, is quasi-periodic. For a sufficiently long time, the phase space point will continuously recur with a high accuracy [3].

Here, we going to use a simple example to demystify this theorem. one can find the mathematical description of the aforementioned theory in Ref.[4]. We know in the case of an ideal gas contained in a box, the volume of phase space is proportional to the volume of the box to the power of a number of molecules.<sup>3</sup> Thus, let us ignore some constant factors and consider a phase space where the volume of the phase space is  $V^N$  (where N is the total number of molecules) and a tiny sub-region of that with volume  $v^N$  (see Figure 2.3). Actually, the small region is a place that is odd to be likely. In other words, the situation where all molecules gather in a small sub-region is very rare. The percentage of the time would you expect the phase point to be in the small region is,

<sup>&</sup>lt;sup>2</sup>There is some ambiguity in who first proposed this idea: due to the so-called "Boltzmann brain" argument some of the community think Boltzmann was the first one who proposed this notion.

<sup>&</sup>lt;sup>3</sup>For more detail see chapter 5 in [2].

$$\frac{v^N}{V^N}. (2.5)$$

By physical intuition, it is clear after an extremely long period of time it will happen whether it is rare to be likely.

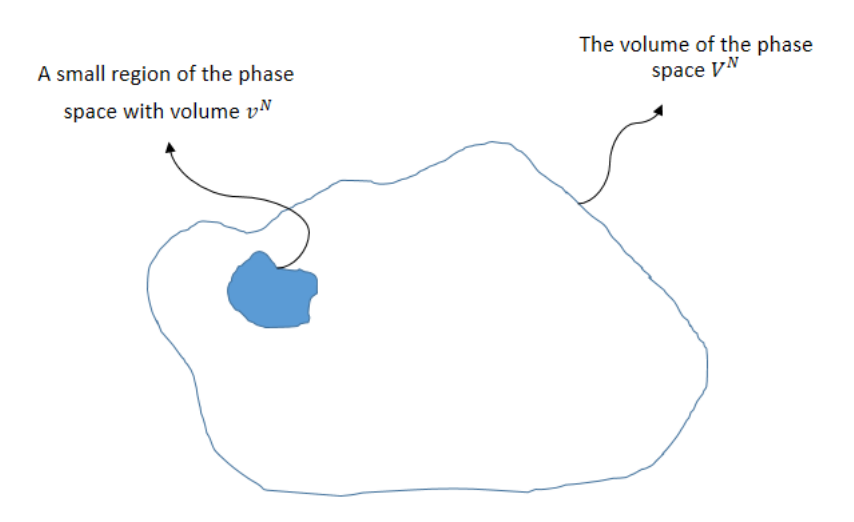


Figure 2.3:  $v_1$  and  $v_2$  are the volume of phase space which are the same

As an interesting fact, based on our definition of entropy in 2.1.2 the logarithm of a volume in the phase space is the entropy of that small region. So we can rewrite (2.5) as a function of entropy,

$$\frac{v^N}{V^N} = e^{-S}. (2.6)$$

#### Quantum version

For a quantum mechanical system with discrete energy eigenvalues, during the evolution of the system, every state will see its initial value in a finite amount of time (this is also valid for values of observable). The proof is given in Ref. [5].

#### 2.1.6 A little bit! information theory

In 1867, James Clerk Maxwell (1831–1879) came up with an interesting puzzle via a thought experiment which is now called Maxwell's demon. This puzzle is solved by a combination of information theory and entropy. The Maxwell demon is a clever example to illustrate

the connection between entropy and information. In the next step, we are going provide a brief review of some essentials of the information theory. For many more details see for example [7].

#### Classical information theory and Shannon entropy

How to quantify the definition of information? Claude Shannon (1916–2001) was the first person who try to answer this question [8]. He found that in the absence of any prior information, the greater the probability of the statement, the less the information content of the statement. Roughly speaking, we are trying to quantify the measure of ignorance or the amount of uncertainty we have about a quantity prior to the measuring process. For instance, "maybe tomorrow will rain" has more content of information in comparison with "tomorrow will rain". Plus, it is natural to assume that information content is additive. Thus, based on the aforementioned, the information content of a statement which is denoted by Q is defined by

$$Q = -k \log P, \tag{2.7}$$

where P is the probability of the statement and k is a positive constant. In some way, the information content is measured by logarithmic unit, and it is convenient to measure that in bits which is  $log_2$ .

We are able to develop this idea to find the **Shannon entropy** or the average information S which is given by

$$S = \langle Q \rangle = \sum_{i} Q_{i} p_{i} = -k \sum_{i} p_{i} \log_{2} p_{i}, \qquad (2.8)$$

where  $Q_i = -k \sum \log_2 p_i$  is a set of the information content of statements with probability P. Here, there is a very interesting point, take  $k = k_B$  in equation 2.8, yes! It is equation 2.3. Now lock at 2.1.3 subsection, we defined entropy in the context of information and thermodynamics. Actually, Rolf Landauer (1927–1999) was the first one who points out that information itself is a physical quantity.

#### Quantum information

The notion of information can be extended to quantum mechanical systems. In the previous section, we deduced that in a classical system, entropy and probability are strongly connected. Based on statistical

<sup>&</sup>lt;sup>4</sup>For details see chapter 14,15 in[6].

quantum mechanics, **density matrix**<sup>5</sup> is associated with probabilities of the outcomes of any measurement performed upon the system. Consider a quantum system that has a number of states  $|\Psi_i\rangle$  with probability  $p_i$ . The density matrix  $\rho_i$  for the system is defined by

$$\rho_i = \sum_i p_i |\Psi_i\rangle \langle \Psi_i|. \tag{2.9}$$

One can show that the expectation value  $\langle \hat{A} \rangle$  of a quantum mechanical operator  $\hat{A}$  is equal to

$$\langle \hat{A} \rangle = Tr[\hat{A}\rho]. \tag{2.10}$$

Note that, for a system with a Hamiltonian  $\hat{H}_0$  that has energy eigenvalues  $E_i$ : In thermal equilibrium at temperature T, **partition function** of a system which is represented by z is defined as follows:

$$Z = Tr[e^{-\beta \hat{H_0}}], \tag{2.11}$$

and the thermal density matrix  $\rho_{th}$  is

$$\rho_{th} = \sum_{i} e^{-\beta \hat{E}_i} |\Psi_i\rangle \langle \Psi_i| = e^{-\beta \hat{H}_0}, \qquad (2.12)$$

where  $\beta = \frac{1}{k_B T}$ . A good discussion about the concept of the thermal density matrix is given in chapter 14 of Ref. [10]. We then replace probabilities with density matrices and take K = 1. Thus for a quantum system, the average information or entropy is

$$S(\rho) = \langle -\log \rho \rangle = -Tr[\rho \log \rho]. \tag{2.13}$$

It is called Von Neumann entropy. As a interesting fact if the eigenvalues of  $\rho$  are  $\lambda_i$ , then the Von Neumann entropy coincide with the Shannon entropy,

$$S(\rho) = -\sum_{i} \lambda_{i} \log \lambda_{i}. \tag{2.14}$$

<sup>&</sup>lt;sup>5</sup>Reference [9] is an excellent elementary book that deals with the basic of quantum information and quantum statistical mechanics.

#### 2.2 Black Holes

After purposing general relativity by Albert Einstein (1879–1955), Karl Schwarzschild (1873–1916) found a spherically symmetric vacuum solution of the Einstein equation which indicates the existence of black holes. But unfortunately, almost nobody accepted that idea for decades. David Ritz Finkelstein<sup>6</sup> (1929–2016) went through the subject. He was the first theoretical physicist who showed that the horizons of a black hole is not singular surfaces. His work influenced the decisions of Lev Davidovich Landau (1908-1968), Roger Penrose (1931-now), and John Archibald Wheeler (1911-2008) to accept the physical existence of the event horizons and the black hole.

Black holes are astonishing, they play a crucial role in theoretical physics. Black holes provide a context in which one can study some underline conflicts in theoretical physics arising due to the inconsistency of quantum mechanics and general relativity. Classically, a black hole can be characterized by its mass, charge, and angular momentum. In this section, we will examine some aspects of black holes and some useful mathematical tools to study them. A detailed argument is given in <sup>7</sup> Refs. [11], [12] and [13] for advanced topics.

#### 2.2.1 Simplest black hole

Imagine a black hole<sup>8</sup> with mass M which is static and spherically symmetric. The solution of vacuum field equations outside the black hole is the **Schwarzschild metric**,

$$-c^2d\tau^2 = ds^2 = -(1 - \frac{2MG}{rc^2})c^2dt^2 + (1 - \frac{2MG}{rc^2})^{-1}dr^2 + r^2d\Omega^2, \quad (2.15)$$

where  $d\Omega^2 = d\theta^2 + r^2 d\phi^2$ , and G is Newtonian constant of gravitation. It would be convenient to take c = 1. For this spherical coordinate, equation 2.15, the point  $r_h = 2GM$  calls **horizon**. The metric at the horizon seems to be singular because, at this point, the coefficient of dr blows up. But  $r_h = 2GM$  is not a true singularity and can be fixed by changing the coordinate system. On other hand, there is a real singularity that exists at r = 0. To distinguish between a **real singularity** and coordinate singularity one can use the famous scalar

 $<sup>{}^{6}\</sup>text{There is a biography of Finkelstein by Leonard Susskind here: "https://www.davidritzfinkelstein.com/blackholes.html"}$ 

<sup>&</sup>lt;sup>7</sup>In the future version, I will add a short review of GR.

<sup>&</sup>lt;sup>8</sup>we will come through the formation of black holes

Kretschmann, which is defined as

$$R^{\mu\nu\rho\sigma}R_{\mu\nu\rho\sigma} = \frac{12r_h^2}{r^6},\tag{2.16}$$

where  $R^{\mu\nu\rho\sigma}$  is Riemann curvature tensor. So, the Kretschmann scalar tells us the real singular point is r=0. Figure 2.4 illustrates schematically the event horizon.

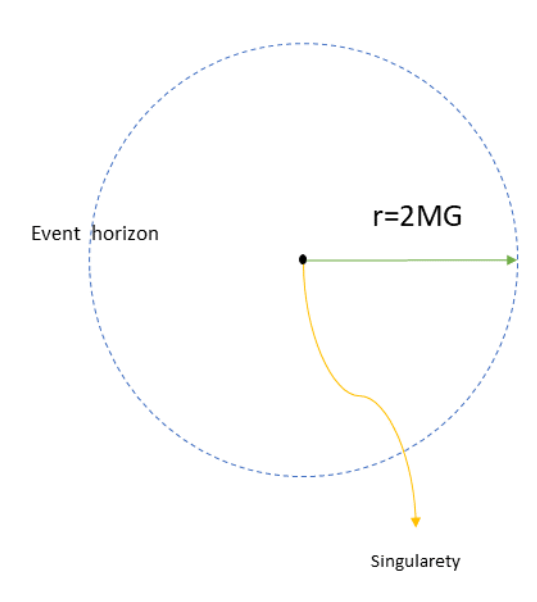


Figure 2.4: Event horizon

#### 2.2.2 The nature of horizon

Schwarzschild black hole and it is horizon property are so generic because it is a very good approximation of other models. The event horizon is a locus of powerful gravitation. If something approaches this circular line, there will be no return even for a light ray! (and so any kind of information!?) Roger Penrose did a great deal of work on horizon and singularities in the context of classical general relativity for details [14]. The singularity of a black hole without the horizon is called a **naked singularity**. Penrose and Stephen Hawking (1942-2018) conjectured that in the classical context, naked singularities do not exist. In a quantum mechanical regime, naked singularities might exist, thus it depends on the theory. More information can be found in [15].

#### Falling into the black hole

Let us imagine an infalling observer near the horizon of the Schwarzschild black hole. In Figure 2.5<sup>9</sup>, an infalling observer sends signals to a distant Schwarzschild observer. For simplicity, we illustrate a black hole as a cylinder and the signals connect the observable causally (based on special relativity light cones).

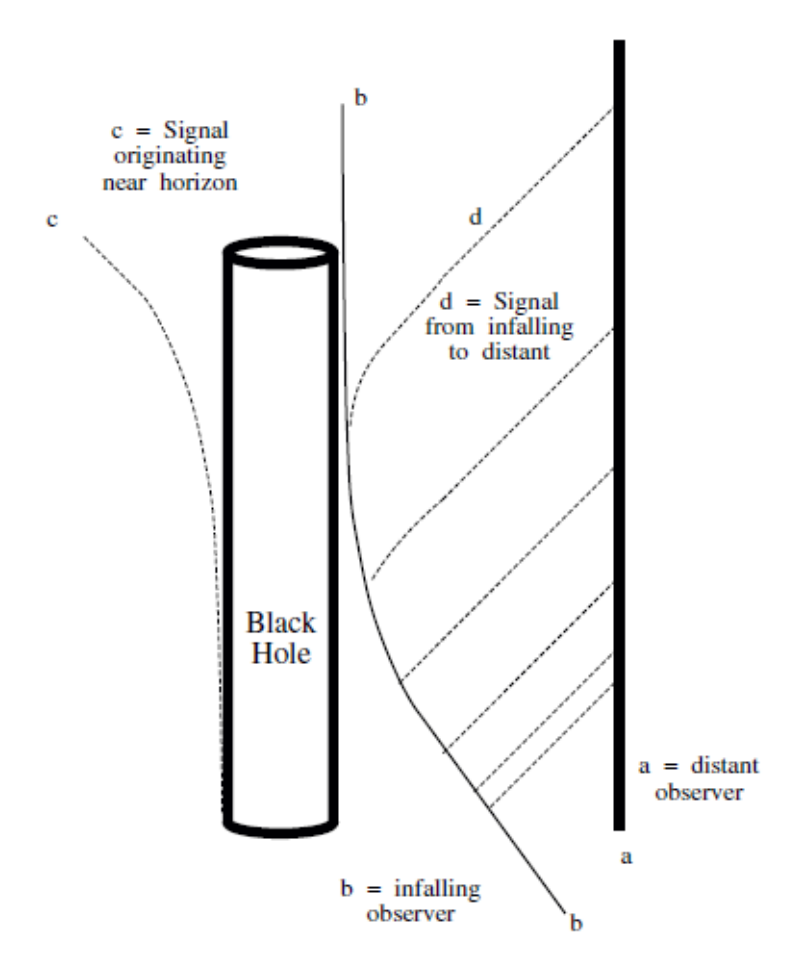


Figure 2.5: Event horizon

Now we are going to write down the principle of least action for an observable which is falling into the black hole radially. The metric and the action are:

$$d\tau = \sqrt{(1 - \frac{2MG}{r})dt^2 + (1 - \frac{2MG}{r})^{-1}dr^2},$$
 (2.17)

$$A = -m \int d\tau, \tag{2.18}$$

where m is the mass of infalling observable and take c=1. Using 2.17 and 2.1 yields

 $<sup>^9{\</sup>rm This}$  figure is adapted from [1]

$$A = -m \int \sqrt{(1 - \frac{2MG}{rc^2})c^2 + (1 - \frac{2MG}{rc^2})^{-1} \frac{dr^2}{dt^2}} dt.$$

So the Lagrangian is

$$\mathcal{L} = \sqrt{(1 - \frac{2MG}{rc^2})c^2 + (1 - \frac{2MG}{rc^2})^{-1}\dot{r}},$$
 (2.19)

where  $\dot{r}$  is the radial velocity. Now we can find the conjugate momentum for r and find the Hamiltonian,

$$\mathcal{H} = \frac{(1 - \frac{2MG}{r})m}{\sqrt{(1 - \frac{2MG}{r}) - \frac{1}{(1 - \frac{2MG}{r})}\dot{r}^2}}.$$
 (2.20)

Because of the conservation of energy. the Hamiltonian does not change with time. Thus, the Hamiltonian is the total energy of the system and is constant, and we take this constant E. Now we can rewrite the equation of 2.20 approximately in the form :

$$\dot{r}^2 \approx (1 - \frac{2MG}{r})^2 - \frac{(1 - \frac{2MG}{r})^3}{E^2}.$$
 (2.21)

Evidently, very close to the horizon when  $r \to 2MG$ , we have:

$$\dot{r} = \sqrt{\frac{r - 2MG}{2MG}} \tag{2.22}$$

This is telling us, as the particle falls toward the Schwarzschild, its velocity gets smaller and smaller instead of accelerating. Briefly,  $r \to 2MG \Rightarrow \dot{r} \to 0$ . This result is valid for a light ray because:

$$d\tau^2 = 0 = (1 - \frac{2MG}{r})dt^2 + (1 - \frac{2MG}{r})^{-1}dr^2$$

$$(1 - \frac{2MG}{r})^2 dt^2 = dr^2$$

$$\dot{r} = 1 - \frac{2MG}{r}.$$

So again,  $r \to 2MG \Rightarrow \dot{r} \to 0$ .

#### 2.2.3 The conflict between Alice and Bob is near the horizon!

First of all, we introduce the hyperbolic coordinate to find the roots of marital problems! between Alice and Bob. By analogy with a circular motion in polar coordinates, we can define some hyperbolic trajectory with uniform acceleration. We will show that the near horizon can be described by the Minkowski spacetime as a good approximation. By changing the coordinate we are able to find the hyperbolic coordinate,

$$X = r \cosh(w)$$
  
 $T = r \sinh(w)$   $\Rightarrow X^2 - T^2 = r^2$ .

For every fixed r, there is a hyperbolic curve that is associated with uniform acceleration. Finally, the metric of this flat space is,

$$ds^2 = -\rho^2 dw^2 + d\rho^2 (2.23)$$

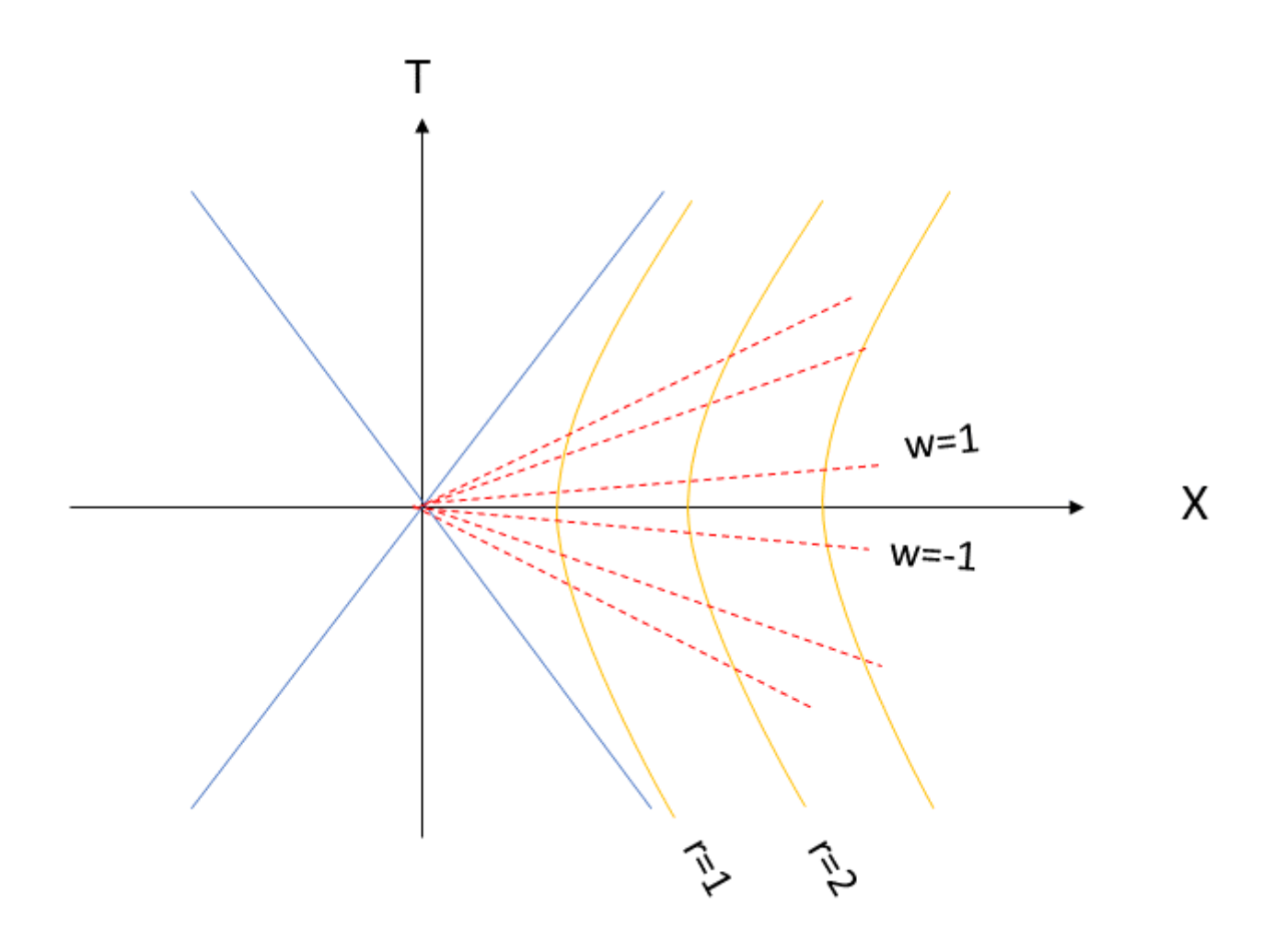


Figure 2.6: Hyperbolic coordinate

As we mentioned near horizon is roughly flat<sup>10</sup>, Thus we can describe black holes in the context of hyperbolic coordinates. In Figure 2.7 the spacetime is divided into four regions by two blue lines, the

<sup>&</sup>lt;sup>10</sup>But for tiny black holes, it is not valid, we will come to that.

region I is called near the horizon.

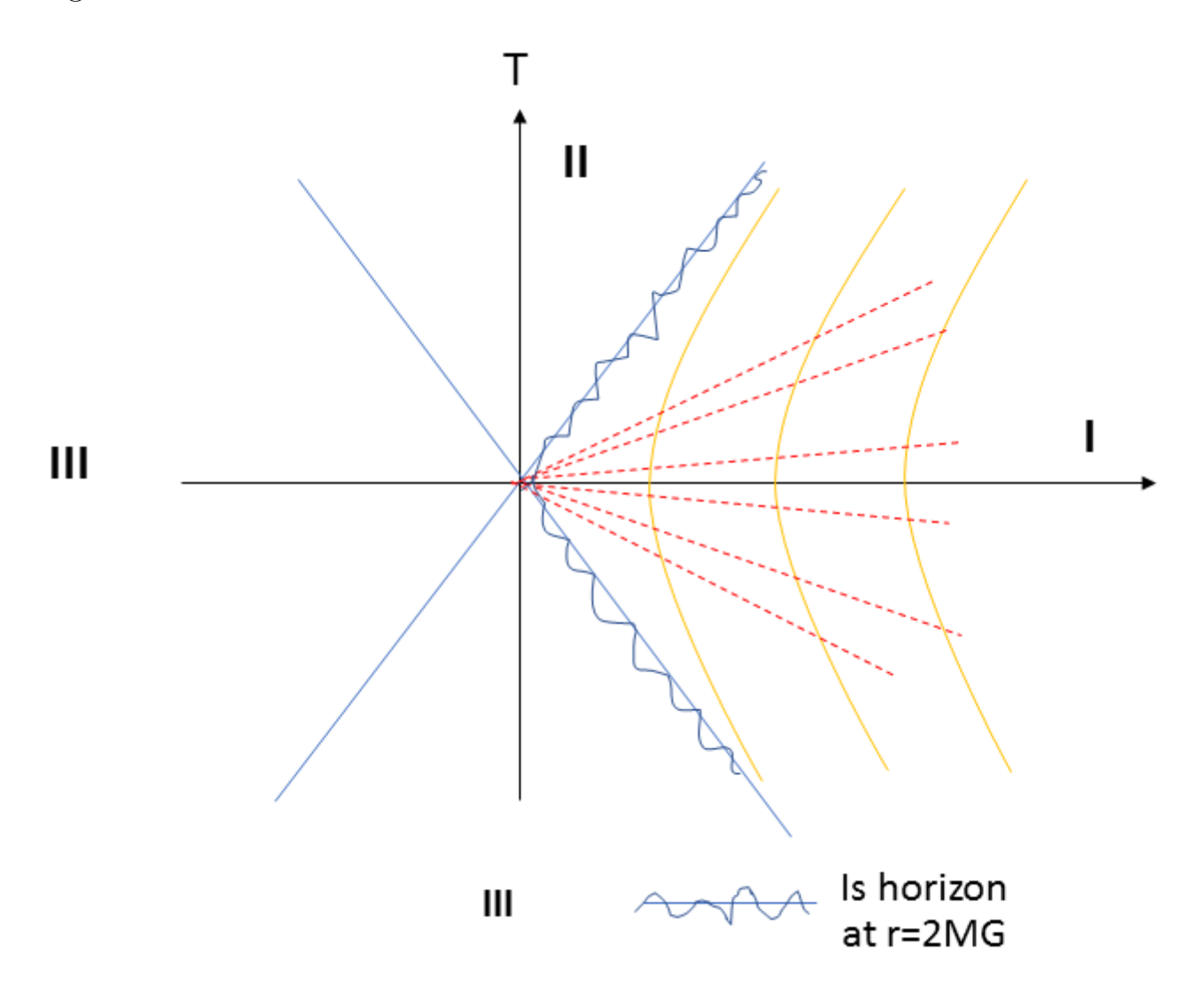


Figure 2.7: Hyperbolic coordinate and the horizon  $\,$ 

Imagine Bob decided to hit the horizon and Alice in a frame with uniform acceleration is trying to send a message as fast as possible. Thus Alice uses light rays. See Figure 2.8, the light rays because of the causal structure are in the shape of 45 degrees light cone. Let us examine how Alice sees Bob. In Figure 2.8 at point S, they separate from each other. Alice to see Bob has to look at the past and so she **never sees Bob cross the horizon** because she has to cut the coordinate axes and it takes an infinite amount of time in Alice's coordinate. But for Bob (Bob as a reference frame) the amount of time it takes to hit the horizon is finite. The final remark is about a conflict between Alice and Bob stating that Alice never believes any information went through the horizon, but bob is negative!

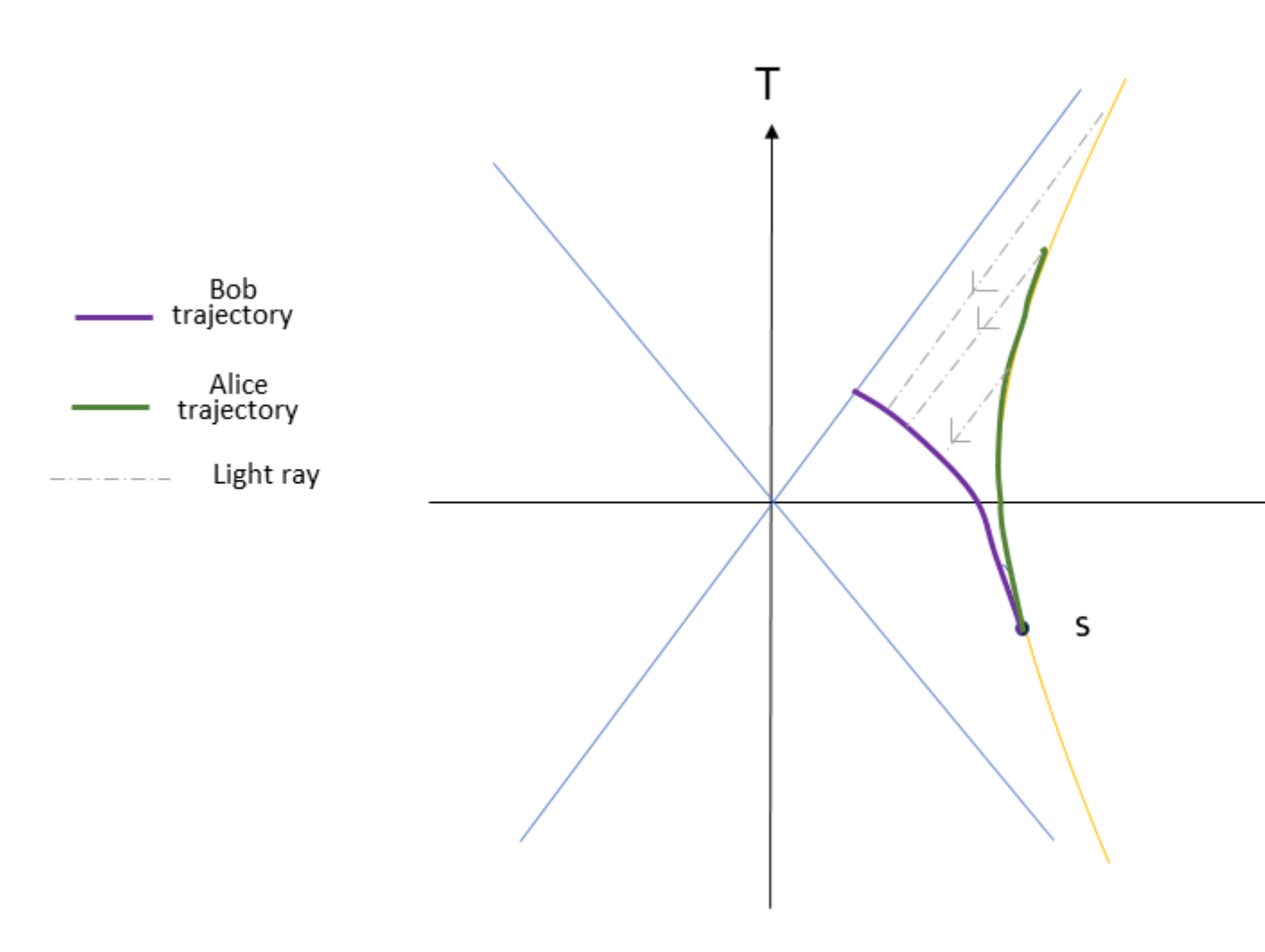


Figure 2.8: Conflict between observers near the horizon

#### 2.2.4 Some useful coordinate systems

In this section, we are going to expand our tools to study black holes.

#### Tortoise coordinate

Remember the Schwrchild metric (equation 2.15), By changing the coordinate as will next be explained, can take the radial-time part of the metric **conformally flat**<sup>11</sup>. We define the tortoise coordinate r\*,

$$\frac{1}{1 - \frac{2MG}{r}}dr^2 = \left(1 - \frac{2MG}{r}\right)(dr^*)^2 = F(r)(dr^*)^2 \tag{2.24}$$

$$d\tau^2 = (1 - \frac{2MG}{r})[dt^2 - (dr^*)^2] - r^2 d\Omega^2.$$
 (2.25)

<sup>&</sup>lt;sup>11</sup>In conformal flat space, the metric is found in the form  $d\tau^2 = F(x)dx^{\mu}dx^{\nu}\eta_{\mu\nu}$ , where  $\eta_{\mu\nu}$  is the Minkowski metric. We are interested in this kind of transformation because they preserve the causal structure of spacetime.

The integration of equation 2.24 gives us the r\*,

$$r* = r + 2MG \log(\frac{r - 2MG}{2MG}).$$
 (2.26)

Note that when  $r \to 2MG \Rightarrow r* \to -\infty$ . So, by this coordinate change, we map the horizon to the minus infinity. Actually, because of that fact, Tortoise takes an infinite amount of time to approach the horizon! it is called the Tortoise coordinate.

#### Rindler coordinate (Rindler space)

Here, we are going to invent a new coordinate to study the near horizon. In Figure 2.9 the proper distance from the horizon is shown by  $\rho$ .

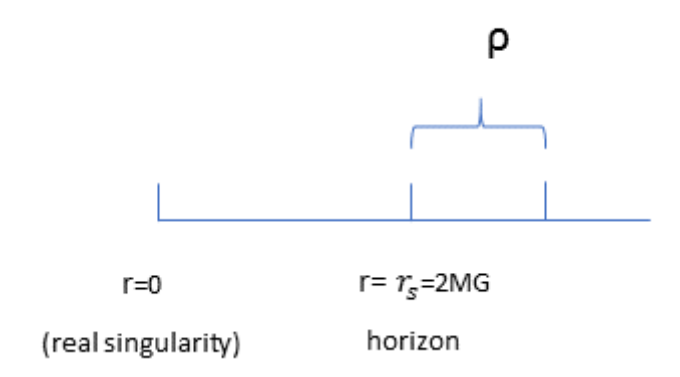


Figure 2.9: Near horizon proper distance

Let us do the calculation,

$$\rho = \int_{2MG}^{r} \sqrt{g_{rr}(r')} dr' = \int_{2MG}^{r} \sqrt{(1 - \frac{2MG}{r'})} dr'$$
 (2.27)

$$= \sqrt{r(r - 2MG)} + 2MG \sinh^{-1}(\sqrt{\frac{r}{2MG} - 1}). \tag{2.28}$$

By rewriting the metric in terms of  $\rho$  and t, we have

$$d\tau^{2} = \left(1 - \frac{2MG}{r(\rho)}\right)dt^{2} - d\rho^{2} - r^{2}(\rho)d\Omega^{2}.$$
 (2.29)

Near the horizon, equation 2.28 give us  $\rho$  approximately,

$$\frac{d\rho(r)}{dr} = \sqrt{\frac{2MG}{r - 2MG}}$$

$$\rho \approx 2\sqrt{2MG(r - 2MG)}. (2.30)$$

So,

$$d\tau^2 \approx \rho^2 \left(\frac{dt}{4MG}\right)^2 - d\rho^2 - r^2(\rho)d\Omega^2. \tag{2.31}$$

For a small angular region of the horizon that we are interested in, it can be replaced by Cartesian coordinates

$$dX = 2MGd\theta \cos\phi - 2MG\theta \sin\phi d\phi$$
  

$$dY = 2MGd\theta \sin\phi + 2MG\theta \cos\phi d\phi.$$
 (2.32)

In the last stage, we define a dimensionless time w,

$$w = \frac{t}{4MG}. (2.33)$$

Finally, the metric is,

$$d\tau = \rho^2 d\omega^2 - d\rho^2 - dx^2 - dy^2. \tag{2.34}$$

Now, we can compare that metric with equation 2.23 to understand this is a flat spacetime in hyperbolic coordinates. Actually, by taking  $T = \rho \sinh \omega$  and  $Z = \rho \cosh \omega$ ,

$$d\tau = dT^2 - dZ^2 - dX^2 - dY^2. (2.35)$$

Note that we prove that the Minkowski spacetime is a very good approximation of the near horizon region.

when we go far from a horizon of a black hole the geometry will change as shown in Figure 2.10. Thus, when you are near the horizon the distance in  $\operatorname{omega}(\rho^2 d\omega)$  depends on  $\rho$ . But when you are far away, it does not depend on  $\rho$ . The main message here is that this is a curved space with curvature near the horizon. So, **the curvature** at the tip of the cigar gets less when the mass is bigger.

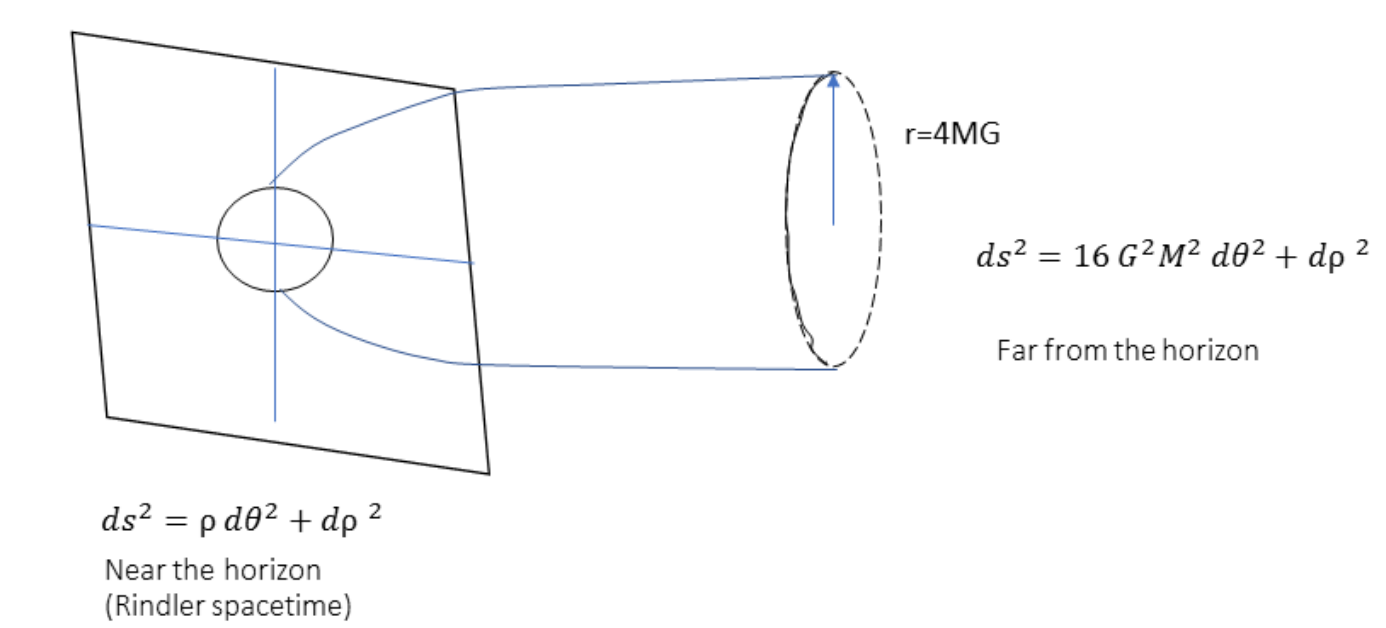


Figure 2.10: Cigar of the near horizon

#### Kruskal-Szekeres coordinate

Based on recent subsections, we can bring the metric of the black hole to this form:

$$d\tau^{2} = F(R)[R^{2}d\omega - dR^{2}] - r^{2}d\omega^{2}$$
 (2.36)

By comparing with equation 2.15 which is the original Schwarzschild metric, we get:

$$R^{2}F(R) = 16M^{2}G^{2}\left[1 - \frac{2MG}{r}\right],$$

$$F(R) dR^{2} = \frac{1}{1 - \frac{2MG}{r}}dr^{2}.$$
(2.37)

Finally, from 2.37 we get

$$4MG \log \frac{R}{MG} = r + 2MG \log \left(\frac{r - 2MG}{2MG}\right) = r *.$$
 (2.38)

So,

$$R = MG \exp\left(\frac{r*}{4MG}\right). \tag{2.39}$$

R and  $\omega$  can be radial parts of flat space in a hyperbolic coordinate. Let us define

$$Re^{w} = V$$

$$Re^{-w} = -U.$$
(2.40)

Evidently,

$$\frac{dV = dR e^{\omega} + dw Re^{\omega}}{-dU = dR e^{-\omega} - dw Re^{-\omega}} \right\} \Rightarrow dU dV = -(dR^2 - R^2 d\omega^2).$$
 (2.41)

The relationship of T and X in the Minkowski spacetime with V and U is,

$$X = R \cosh w = V - U$$
  

$$T = R \sinh w = V + U.$$
(2.42)

Based on 2.41 we have the radial-time part of the metric in this form:

$$d\tau^2 = F(R)dUdV. (2.43)$$

The coordinate of (V, U) is shown in Figure 2.11<sup>12</sup>, in this diagram region I is called the near horizon, and every observer which is in this region, because of the 45 degree light cones never cut  $H^-$  (it is called extended past) and it will cut  $H^+$  (it is called future horizon). Region II is behind the horizon when the observer passes  $H^+$ , r is shrinking and when r goes zero it hits the singularity.

<sup>&</sup>lt;sup>12</sup>I used the TikZ.net package to draw the picture.

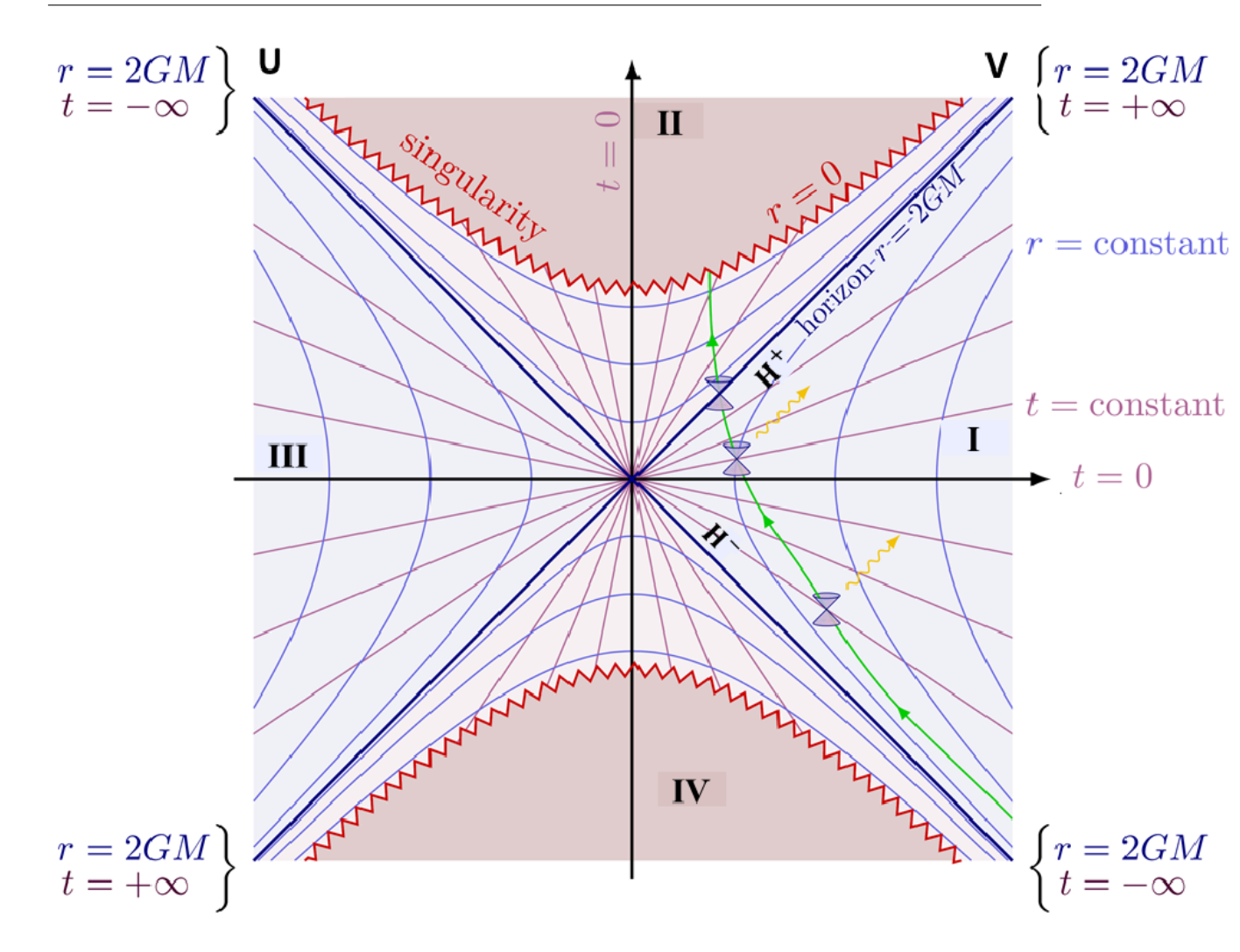


Figure 2.11: Kruskal-Szekeres coordinate

#### 2.2.5 Carter-Penrose diagrams

When the geometry of spacetime has rotational symmetry (or spherical symmetry) which means that the same in every direction it is convenient to use Carter–Penrose diagrams. In this system we do not care about angles, what we care about is how things vary as we move away from the center(the radial direction). We going to compactify an infinite two-dimensional geometry of spacetime on the finite plane. Maybe before starting, we should ask how it could be possible. we owe Georg Cantor(1845–1918) one! This genius mathematician by a simple argument proved that always we can put an infinity between two real numbers (Cantor's diagonal argument).

Here, we going to do a new coordinate change in the two-dimensional surface of fixed angular coordinates. Our new coordinate is defined as follows which is shown in Figure 2.12,

$$T + R = T^{+}$$
  
 $T - R = T^{-}$ . (2.44)

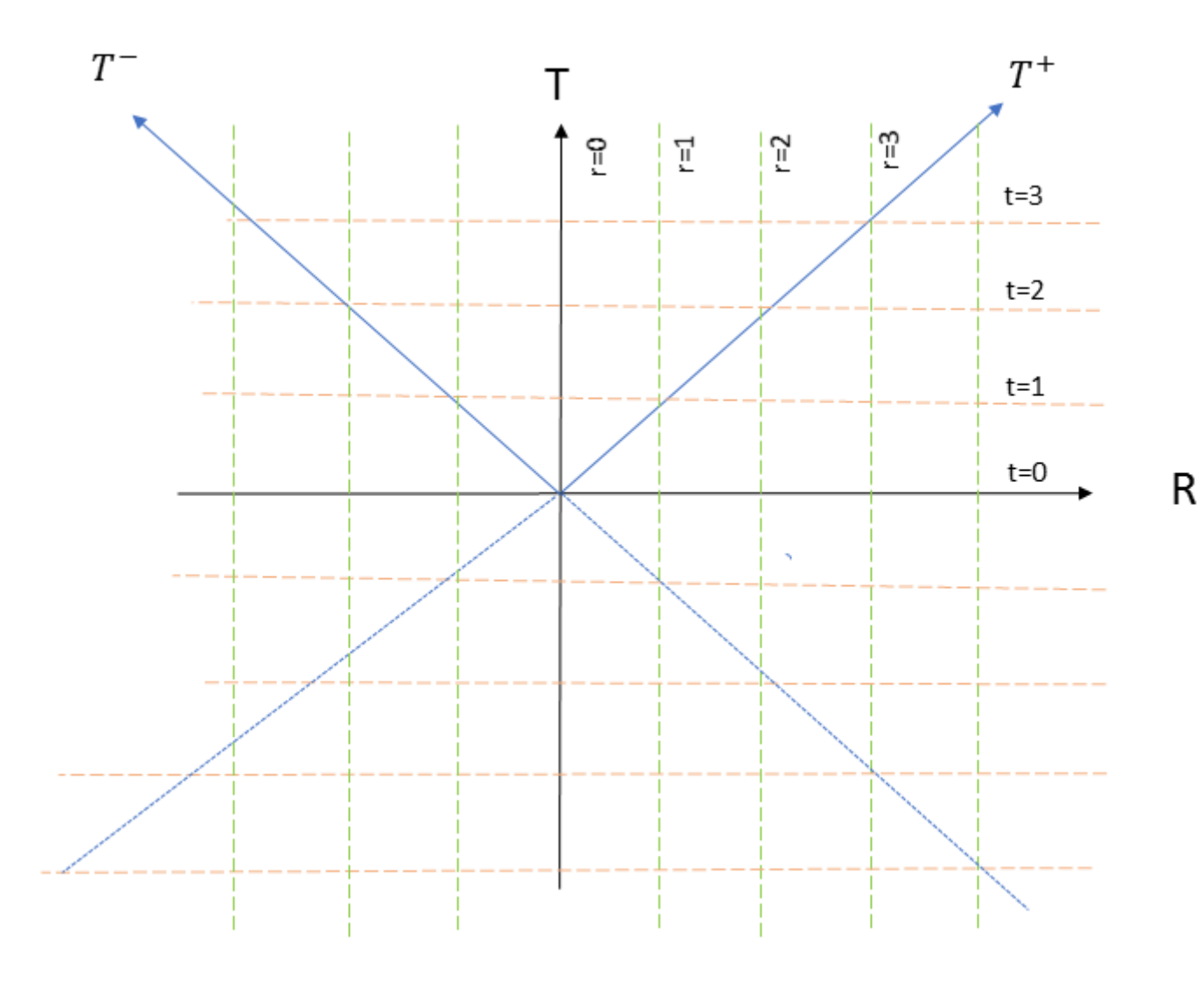


Figure 2.12: Light cone coordinate

Finally, we use this transformation to map the entire infinite spacetime region  $-\infty \le T \le +\infty, 0 \le r \le +\infty$  to a finite portion of the plane as follows:

$$Y^{+} = F(T^{+}) = tanh(T^{+})$$
  
 $Y^{-} = F(T^{-}) = tanh(T^{-}).$  (2.45)

Thus, we compactify the spacetime as shown in Figure 2.14, and the diagram with more detail is shown in Figure  $2.13^{13}$ .

<sup>&</sup>lt;sup>13</sup>I used the TikZ.net package to draw the picture.

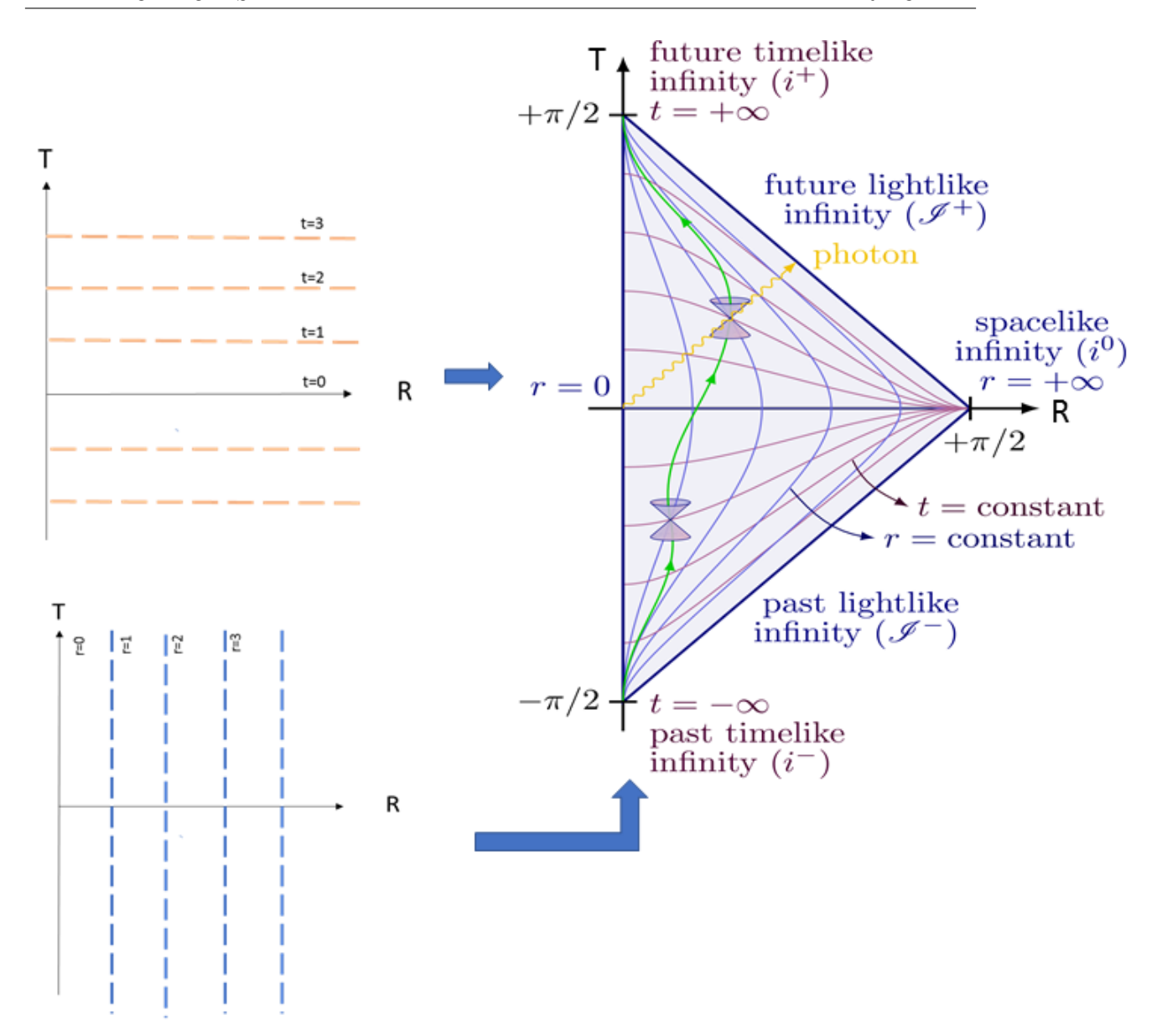


Figure 2.13: Compacted spacetime between  $Y^+$  and  $Y^-$ , more detail

It is practical to bring Kruskal-Szekere diagrams in the form of Carter–Penrose diagram, and so we will have Figure 2.15<sup>14</sup>.

As an interesting fact regions, III and IV together can be another kind of black hole that is connected to the black hole in regions I and II by a wormhole. Wormholes were not interesting to the physicist for decades because they seem to be unreal. Nevertheless, Lenord Susskind(1940-now) and Juan Maldacena(1968-now) propose a revolutionary idea on how to use wormhole and entanglement to make the connection between Quantum mechanics and general relativity [16].

<sup>&</sup>lt;sup>14</sup>I used the TikZ.net package to draw the picture.

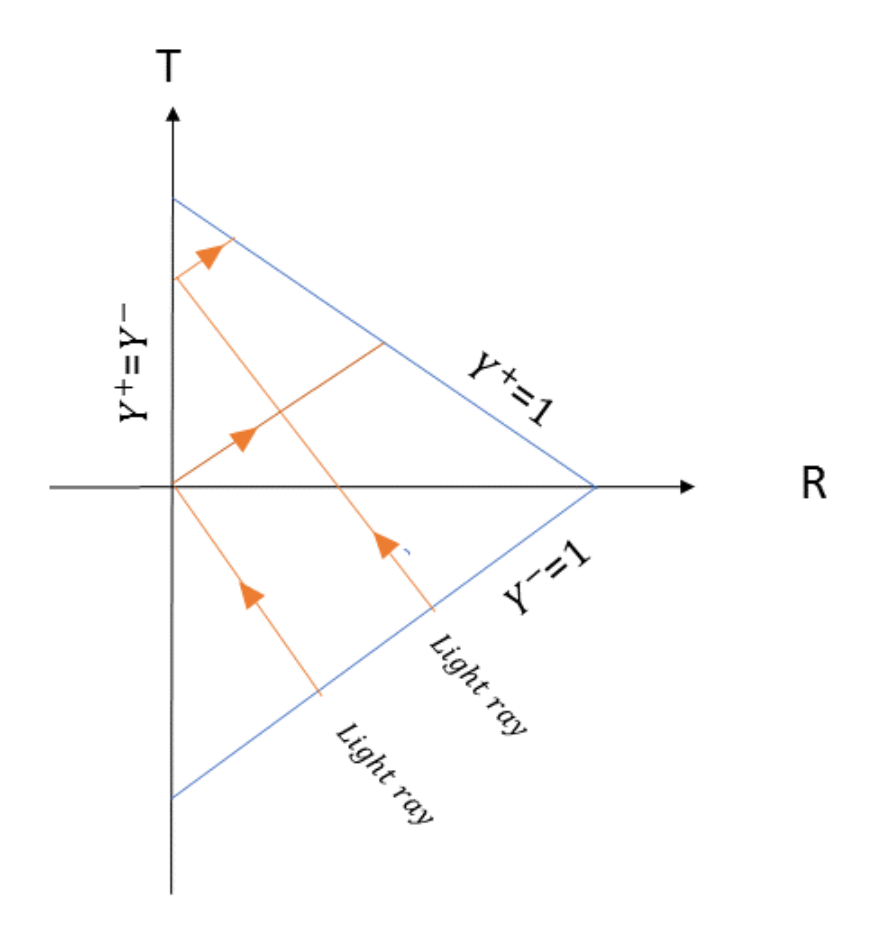


Figure 2.14: Compacted spacetime between  $Y^+$  and  $Y^-$ 

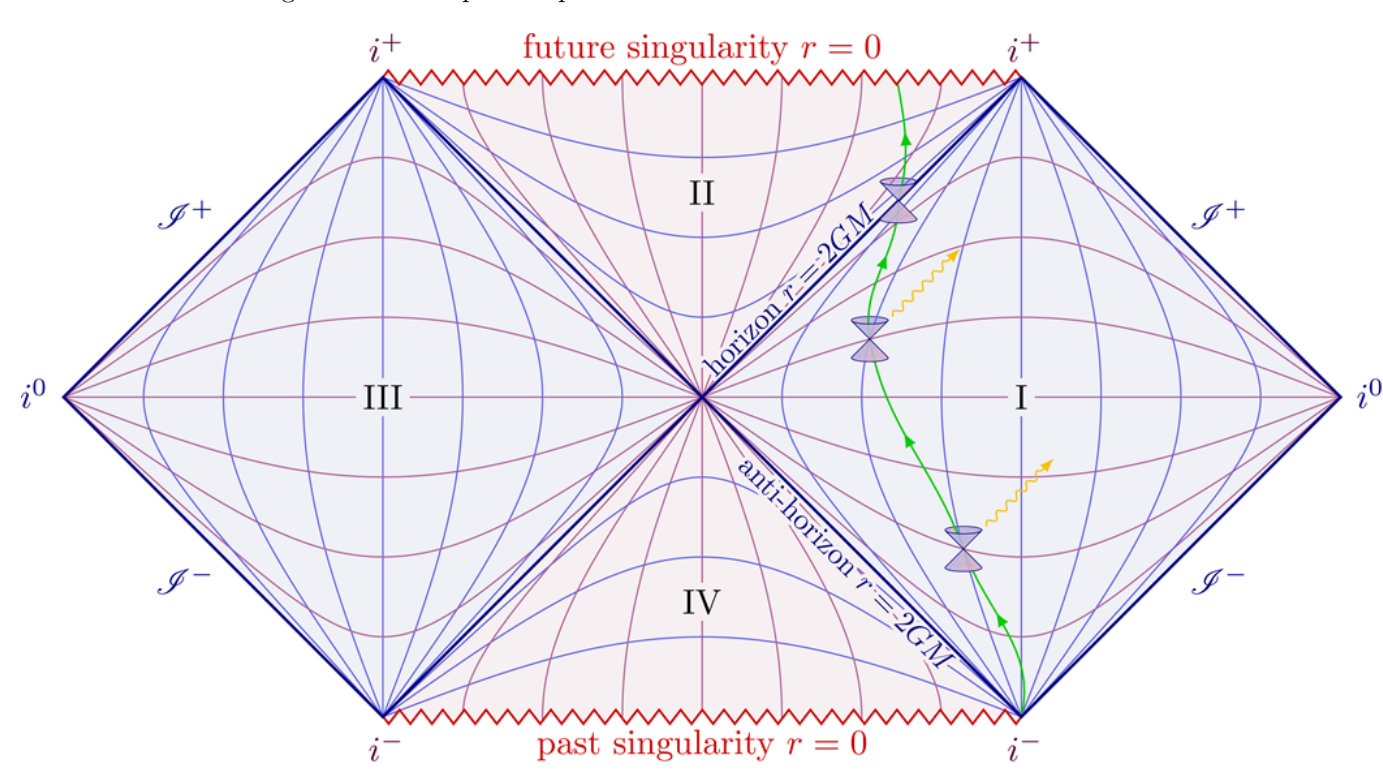


Figure 2.15: Extended Penrose diagram for Schwarzschild black hole.

#### 2.2.6 Formation of black holes

From classical gravity (Newtonian gravity), we know the interior of a shell of mass of matter is like flat spacetime, and the exterior looks like Schwarzschild black hole<sup>15</sup>. Based on Birkhoff's theorem this theory is true in general relativity. The simplest model of the formation of black holes is the collapsing spherical shell of massless matter (like photons).

Now we going to see how is empty spacetime with in coming shell of radiation, in the Penrose diagram (see Figure 2.16).

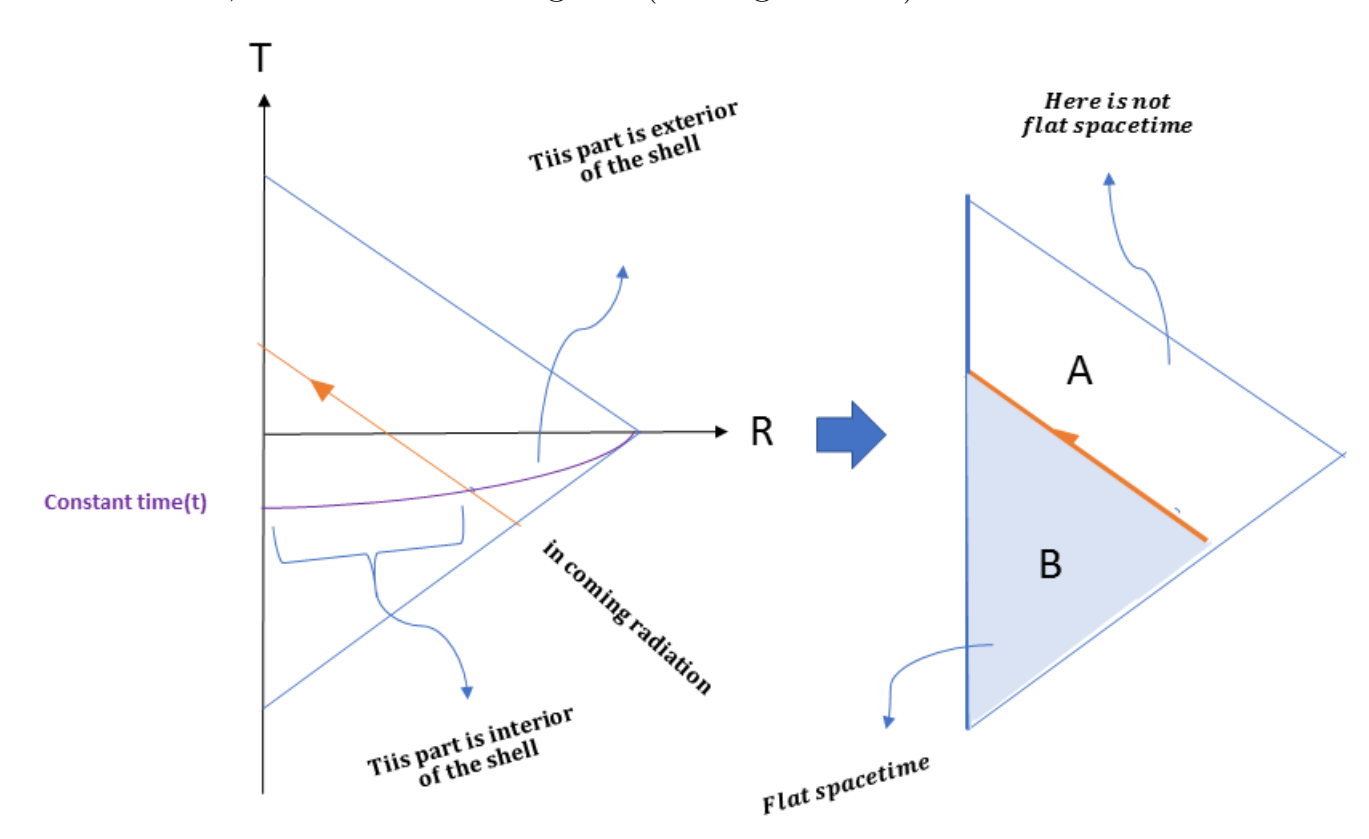


Figure 2.16: Shell of radiation, in the Penrose diagram.

Region A in Figure 2.16 is not flat spacetime. On the other hand, the Penrose diagram was made for flat spacetime. Thus, we have to replace region A with a part of the Schwarzschild black hole which is region C (the green region) in Figure 2.17. By this replacement, we will find Figure 2.18.

 $<sup>^{15}</sup>$ The proof and details can be found in chapter 5 in [17]

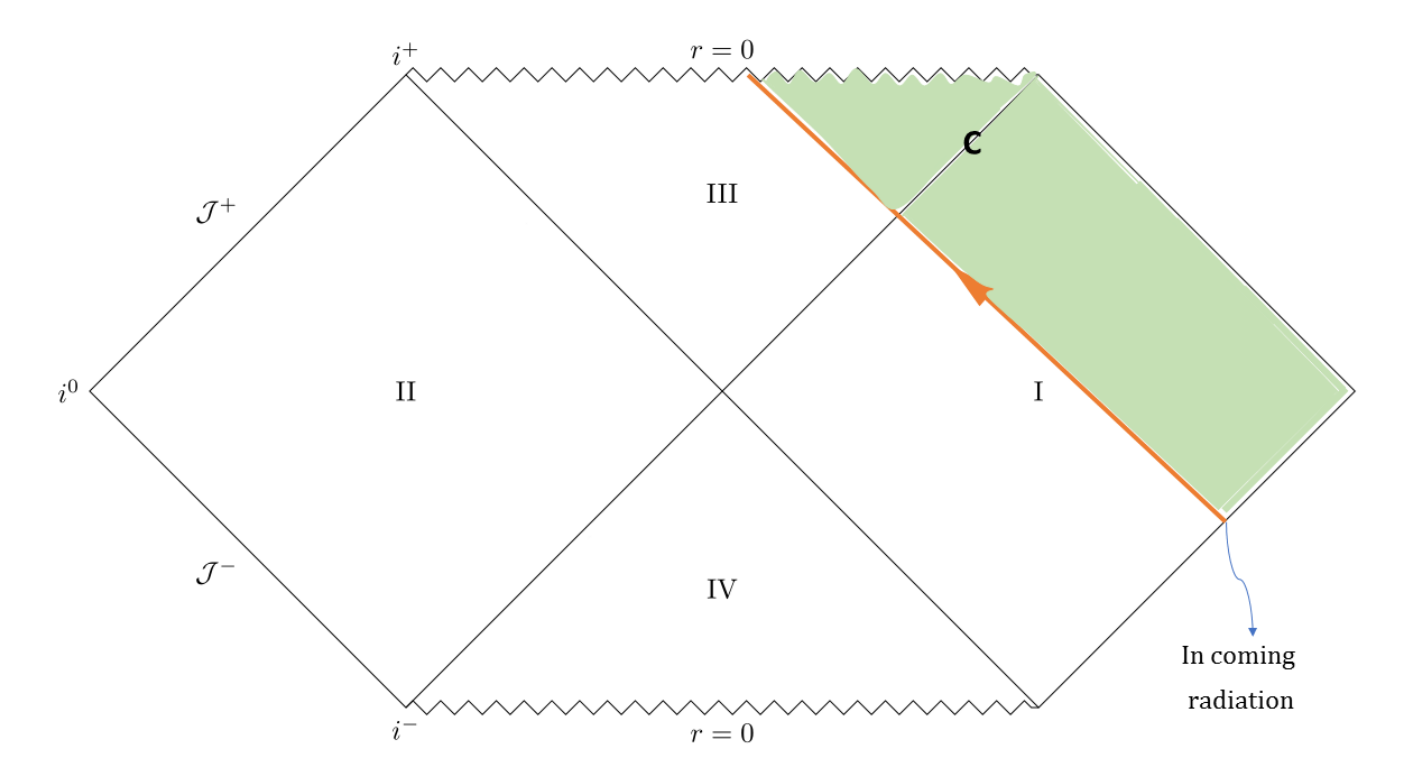


Figure 2.17: Shell of radiation, in the whole of Penrose diagram.

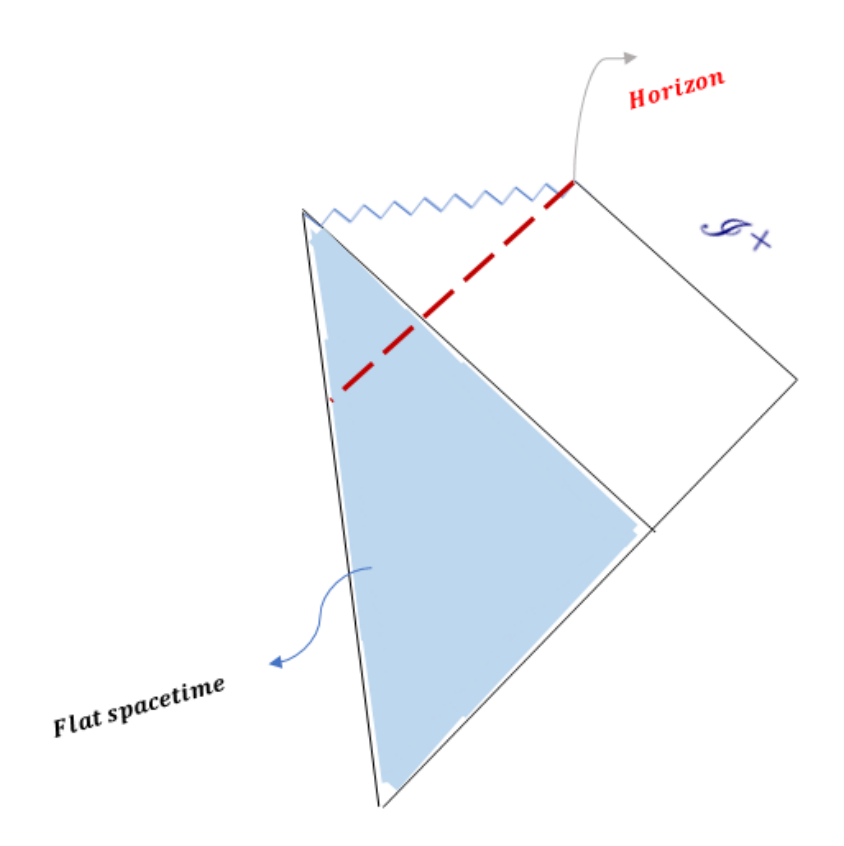


Figure 2.18: The geometry of a black hole that is formed by an infalling shell

#### 2.3 Holography and Black Holes Thermodynamics

Up to now, we review some properties of the horizon. Now, it is time to go through the subject of black holes in the context of thermodynamics. Jacob Bekenstein (1947-2015) and Stephen Hawking proposed an idea due to the assumption of the black hole as a black-body, and it follows that defines black-body radiation, entropy, and temperature for black holes.

#### 2.3.1 Entropy of a black hole

Here to derive the entropy of a black hole which is called Bekenstein-Hawking entropy [18], we going to drop in bits of information to form a black hole. First of all, we need to define our fundamental units of information bits. The process is asking did the photon go in or not, actually, every bit is the answer to a yes-no question. We get the wavelength of a photon is equal to Schwarzschild radiance. Thus, because of the uncertainty, principle every photon represents one bet of information and we have:

$$\lambda = \frac{2MG}{c^2}$$

$$E = pc,$$
(2.46)

where, E, and p are wavelength, energy, and momentum of a photon. Plus, we take the radiance of spherical coordinate one(r=1). Form quantum mechanics  $p=\frac{\hbar}{\lambda}$  and so  $E=\frac{C^3\hbar}{2MG}$ . In subsection 2.1.3 we mentioned the temperature is the change in entropy of systems if you add one bit of information. On the other hand the  $E=Mc^2$ , it follows that:

$$\delta Mc^{2} = \frac{c^{3}\hbar}{2MG}$$

$$or$$

$$\delta M = \frac{c\hbar}{2MG},$$
(2.47)

this is the minimum change in the mass when you add one bit of information. We know  $R_s = R = \frac{2MG}{c^2}$  or  $\delta R = \frac{2G\delta M}{c^2}$ , Using equation 2.47, finally, we obtain

$$\delta R^2 = 2R\delta R = \frac{4G\hbar}{c^3} = \delta A, \qquad (2.48)$$

where A is the horizon area. Thus, the entropy of a black hole is

$$S_{BH} = \frac{Ac^3}{4G\hbar} = \frac{\mathcal{A}}{4},\tag{2.49}$$

where BH is Bekenstein–Hawking and  $\mathcal{A}$  is the horizon are in Planck unit. The horizon area is  $A=4\pi R^2=\frac{16\pi G^2M^2}{c^4}$  it follows that

$$T = \frac{\hbar c^3}{8\pi k_B GM},\tag{2.50}$$

where T is called the Hawking radiation temperature.

#### 2.3.2 Luminosity of the black holes

The Stefan–Boltzmann law for black holes as an ideal black-body is

$$-\frac{dE}{dt} = AT^4, (2.51)$$

where  $-\frac{dE}{dt}$  is the energy that is emitted per time. By taking  $c=G=\hbar=1$  we obtain

$$-\frac{dM}{dt} = AT^4 \approx R_s^2 T^4, \tag{2.52}$$

and  $T \approx \frac{1}{R_s} \approx \frac{1}{M}$ , thus

$$-M^{2} \frac{dM}{dt} \approx 1$$

$$or$$

$$-\frac{dM^{3}}{dt} \approx 1,$$
(2.53)

where it indicates that the cube mass of black holes is proportional to the evaporation time.

#### 2.3.3 Sting theory and black holes

In this section, I will focus on the transition between string and black holes <sup>16</sup>. This section is based on [20] by Leonard Suskind and one of his lectures <sup>17</sup> at Stanford. Recent developments and technical issues can be found in [21]. Plus, I explain some fundamental notions in the string theory which are necessary, a complete description can be found in Ref [22].

<sup>&</sup>lt;sup>16</sup>For a review of black holes in the context of string theory see Ref [19]

<sup>&</sup>lt;sup>17</sup>https://theoreticalminimum.com/courses/cosmology-and-black-holes/2011/winter

We can start with this question: "what the microscopic objects are that carry the entropy of the black hole based on string theory?".

The unit of length that is important for the structure of string theory is different than the unit of length that is important to the structure of gravity. Note that we take  $c = \hbar = 1$ .

#### Gravitational length

The gravitational length is Planck length:

$$l_p = \sqrt{\frac{G\hbar}{c^3}} = \sqrt{G}.$$
 (2.54)

#### String

Consider a typical string and heat it up. Thus it will wiggle all over the place (Figure 2.19). But, the size of the wiggles would be a particular characteristic size scale. The wiggles were never on a smaller than the string length scale.

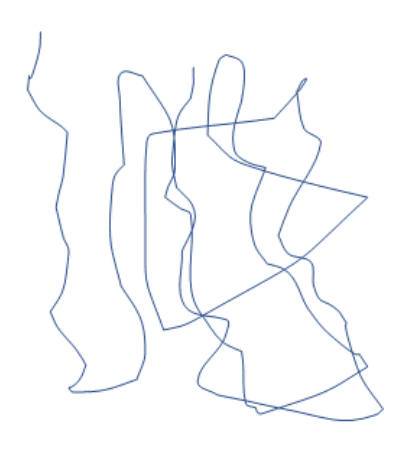


Figure 2.19: Heated string

#### String coupling constant

The string coupling constant is the probability that if a string crosses itself, it breaks (Figure 2.20). Also, it is the amplitude for oscillating, whatever it is doing to emit a graviton.

The Newton constant and string coupling, g, are related by,

$$g^2 l_s^2 = G. (2.55)$$

So,

$$g^2 l_s^2 = l_p^2, (2.56)$$

Where  $l_s$  is the length of the string.

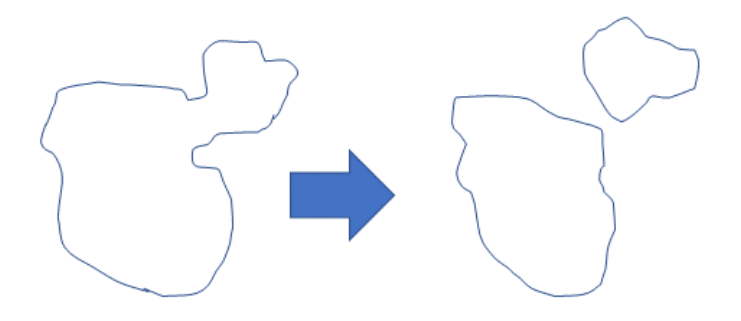


Figure 2.20: Breaking a string

#### Free string entropy

First of all, the entropy of a black hole, based on our new units is 18,

$$S_{BH} = \frac{A}{G} = \frac{R_s^2}{G} = M^2 G = \frac{A}{l_p^2} = M^2 l_p^2$$
 (2.57)

Now, we are going to use a crude but effective model to estimate vibrating string entropy. Consider a big tangled mass, the entropy of that is the number of configurations that are hard to tell apart.

First, oversimplify the space as some piece of lattice, and create strings by connecting parts as shown in Figure 2.21.

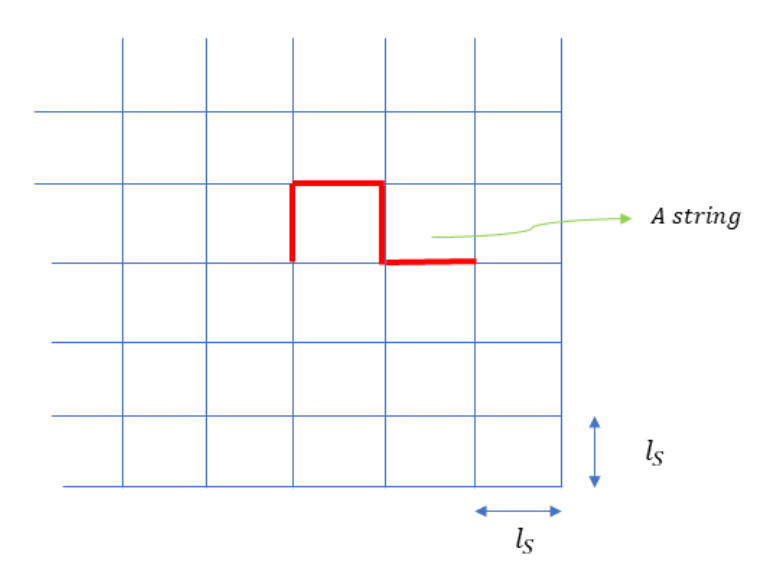


Figure 2.21: Depict the excited string as a closed random walk on a lattice in the plane.

Every link in Figure 2.21 has four configurations in every step of the random walk to create a sting. Thus all of the possible string

 $<sup>^{18}</sup>$ We will come to that why ignore the numerical constant factor (1/4) on the entropy of a black hole.

configurations for a string with n link are:

$$\underbrace{4\times\cdots\times4}_{n\text{-times}}=4^n.$$

So, the order of magnitude of the string entropy is

$$S_{st} = \log_2 2^{2n} \approx n$$

, and if the length of string is L, so  $L = nl_s$ , it follows that

$$S_{st} = \frac{L}{l_s}. (2.58)$$

We have for the mass of every link:

$$M_{link} = \frac{1}{l_s},$$

so the mass of the hole string is:

$$M_{st} = \frac{n}{l_s} = \frac{L}{l_s^2}.$$

We can rewrite the entropy of the string as follow:

$$S_{st} = l_s M_{st}. (2.59)$$

But we had  $S_{BH} = M^2G$ . Thus, we have to change  $S_{st}$ !

#### A crude model

Let us consider an excited (ball of) string that is shrinking. In other words, g is varied, and in the following way which is shown in Fig 2.22 the ball of mass can be a black hole:

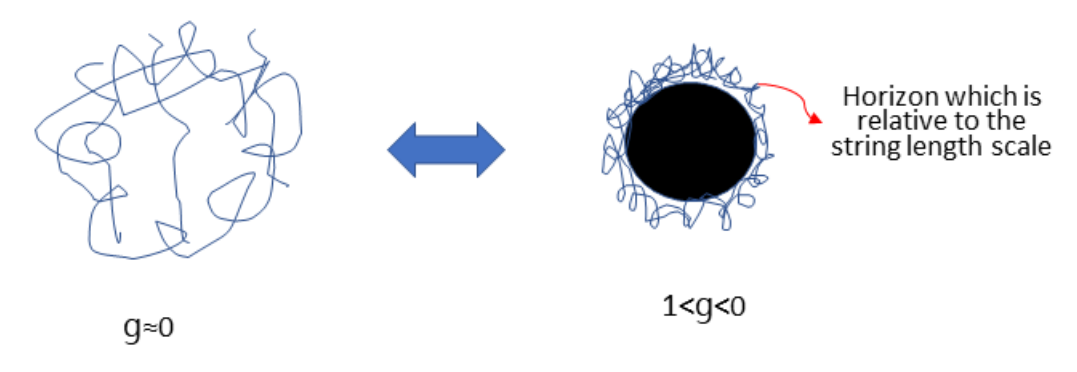


Figure 2.22: Create a black hole by Varying g.

We define the transition point as the point of separation between the ball of string and the black hole, the transition is happening when  $R_s = l_s$ . If the Schwarzschild black hole radius is smaller than the little loops of string (around the black hole) it does not mean anything to say it is a black hole.

$$R_s = l_s \Rightarrow M l_p^2 = l_s.$$

Thus, in the transition point, we have:

$$Mg^2l_s^2 = l_s \Rightarrow Mg^2l_s^2 = 1.$$
 (2.60)

To create a black hole, we can turn it into one string, two strings, etc. But we know that the overwhelming majority of configurations is a single string (the maximum entropy). Plus, the process of creating a black hole can be done slowly. In other words, the process is adiabatic invariant and the entropy does not change. The entropy of a black hole sting depends on the mass but is not dimensionless, so we can write:

$$S = F(M, l_p) = F(M, g l_s),$$
 (2.61)

where F is just a generic function.

Consider a black hole with  $M_0$  and  $g_0$ . As we decrease g the negative gravitational energy disappears, so the mass of strings increases. On the other hand, the entropy of the system is invariant and because  $l_s$  is fixed, we have:

$$M_0 g_0 = M_1 g_1, (2.62)$$

where  $M_1$  and  $g_1$  are amounts of g and M after a finite amount of time in the adiabatic process.

We can plot equations 2.61 and 2.62 as shown in Figure 2.23 <sup>19</sup>. Now, we want to find the intersection point(\*) of two curves in Figure 2.23, so we have:

$$\left. \begin{array}{l} M_*g_* = M_0g_0 \\ M_*g_*^2 = \frac{1}{l_s} \end{array} \right\} \Rightarrow M = M_0^2 g_0^2 l_s.$$

So

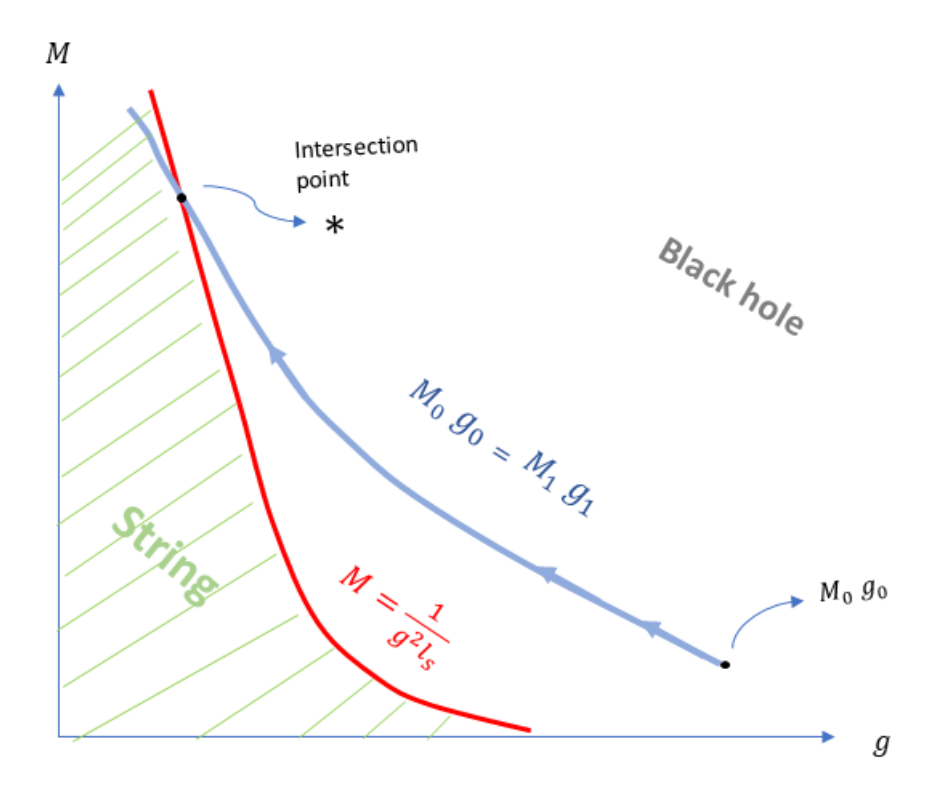
$$M_*l_s = M_0^2 g_0^2 l_s,$$

it follows that

$$M_*l_s = M_0^2 G_0 = S_* = S_0. (2.63)$$

Thus, we showed the entropy of a black hole is the same as mentioned in equation 2.57. But it was not powerful enough to

 $<sup>^{19}</sup>$ Note that the asymptotic behavior of two curves needs correction, but for our purpose, it can be ignored.



Figure~2.23:~. The red curve is the transition line between the black hole and the string. The blue curve is the line which all along that entropy is constant.

determine the numerical constant factor  $(\frac{1}{4})$ . To derive the numerical factor we provide a very mathematically sophisticated version that had a great deal of symmetry, etc.

#### 2.3.4 Holographic principle

The holographic principle is an implication of the debate about information loss in black holes<sup>20</sup>. The proposal of the holographic principle is referred to by Suskind and Hooft in these two famous papers, [25], and [26]. The review of the holographic principle in reference [18] is very interesting because the author attempts to cover various issues on the subject.

Here, the right question is not "what is the entropy of a system?", the question is, "what is the maximum entropy that a system can have?".

Thus, the notion is the maximum entropy. The maximum entropy is infinite for many mathematical systems. consider a simple system which can be described as a system that is built out of qubits. A qubit is a yes/no description (actually it is a quantum bit). We could take

<sup>&</sup>lt;sup>20</sup>See for example, [23], and [24].

a room as our sample space, we could subdivide it into cells to make a cubic lattice out of it. Let us simplify the discussion and suppose everything in the room was made out of one kind of  $atom^{21}$ . We are going to subdivide the room into a large number of cells. Each cell is about as big as one atom. The only question that we can ask about a cell is, is there an atom in it or not? We can make up a lot of different kinds of configuration atoms. The number of configurations that we can make is clearly  $2^{V/V_{atom}}$ , where V and  $V_{atom}$  are the totals volume of the sample space and the volume of a cell.

Thus, the maximum entropy of the system,  $S_{max}$ , is

$$S_{Max} = log \ 2^{\frac{V}{Vatom}}. \tag{2.64}$$

 $S_{max}$  is proportional to the volume, so it is proportional to the number of the basic description of the system which is called **the number of degrees of freedom**.

The statement maximum entropy is proportional to the volume is one of the very general features of nature [1].

Based on the holographic principle, For an incoming shell of mass or radiation that is forming a black hole, the entropy of this system can not be more than black hole entropy in comparison with every possible configuration of the system. This is illustrated in Figure 2.24.

In other words, the number of degrees of freedom of a region of space and everything that can be described in a region of space is no bigger than the area of the bounding surface of that region measured in the plunk unit.

Also, the holographic principle can be stated, **Any region of space** can be described by the collection of degrees of freedom which are one per Planck area on the boundary of the region[1].

<sup>&</sup>lt;sup>21</sup>Note that this is an oversimplified model.

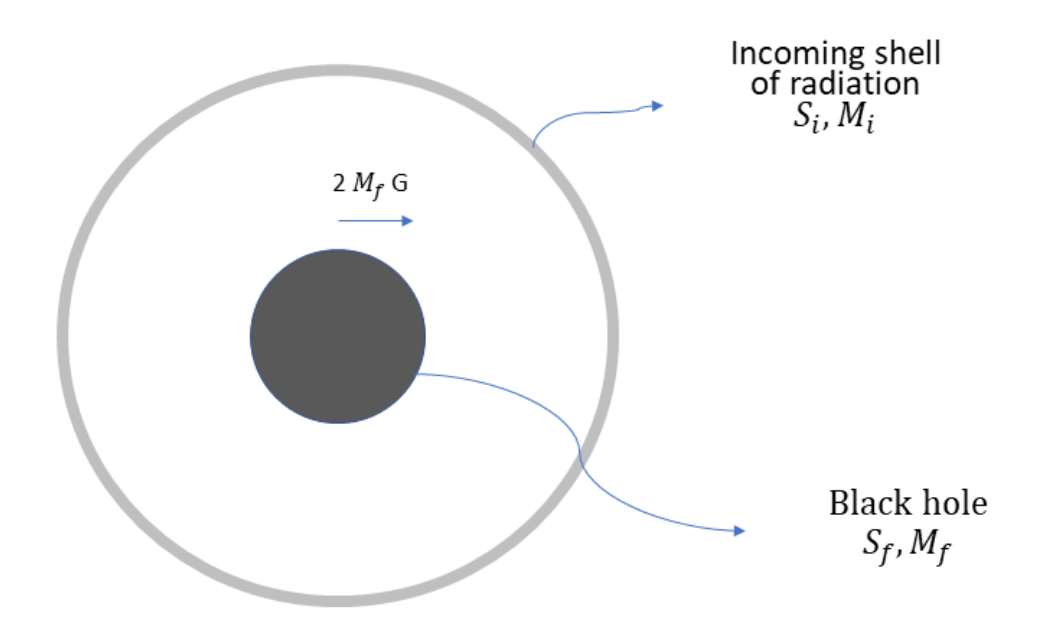


Figure 2.24: Here  $M_i < M_f, S_i < S_f$ , and  $S_f = S_{Max} = \frac{A}{4} > S_i$ .

## Chapter 3

# AdS/CFT and Critical Phenomena

### 3.1 AdS/CFT Correspondence

In this section, I am going to underline an elementary description of the "anti-de Sitter/conformal field theory correspondence" as preparation to use the application of this duality. A intricate review can be found, for instance see [27], [28], [29], [30], and [31].

#### 3.1.1 A qualitative description of AdS/CFT

The AdS/CFT correspondence was first proposed by Juan Maldacena [32]. This paper is the most highly cited in theoretical physics. So, it is clear the paper is so important, see Figure 3.1<sup>1</sup>.

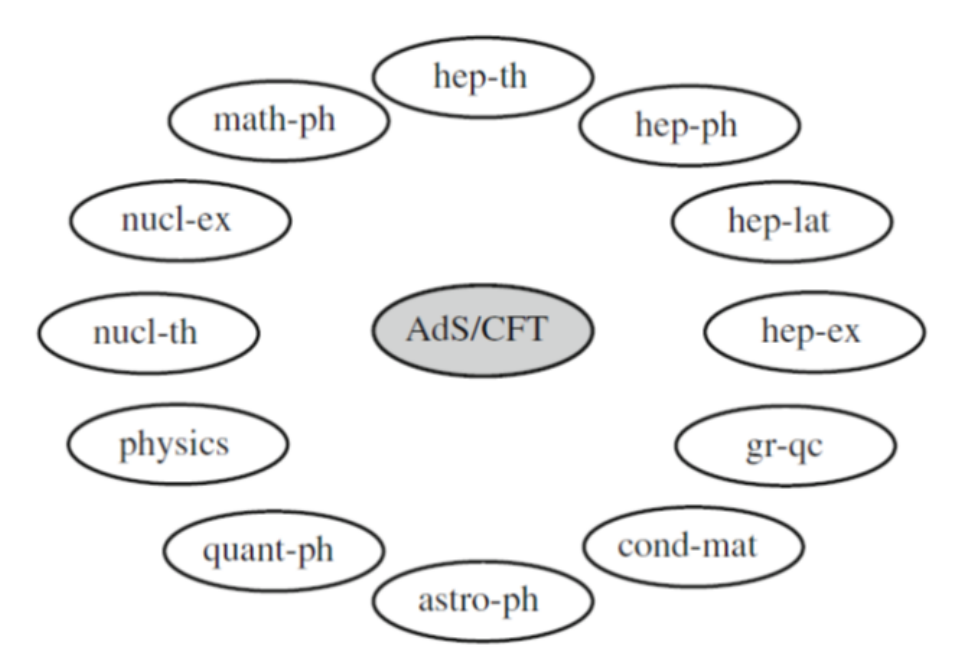


Figure 3.1: The AdS/CFT duality spans all physics arXivs!

<sup>&</sup>lt;sup>1</sup>The figure is adapted from [31].

In chapter 2, we mentioned that based on the holographic principle there is a relationship between the degrees of freedom of the system in the bulk and boundary of the system. One of the implications of the holographic framework which comes out of string/M-theory is AdS/CFT. Thus there should be a correspondence between the bulk and boundary of the system. One piece of the puzzle which is associated with the bulk is AdS space in five dimensions. The last piece of the puzzle is conformal field theory which is associated with the boundary. Actually, the duality is between two theories:

- 1) Five-dimensional gravity.
- 2) Super Yang-Mills theory defined on the boundary.

Where Super Yang-Mills is a theory of particle interaction with supersymmetry.

Thus, the Yang-Mills theory can be colloquially thought of as a hologram on the boundary of the real five-dimensional space where the five-dimensional gravitational physics is taking place[33].

#### 3.1.2 AdS space

Normally, it does not mean having a ball-like region with a boundary in general relativity. But, Anti-de Sitter space is a ball-like space with a negative cosmological constant. Thus, AdS is a suitable framework to study the Holographic principle and its implications.

We are interested in a particular AdS,  $AdS(5) \otimes S(5)$  (see Ref [34] and [35]). It is a 10-dimensional product and it has two factors, which one is the 5-dimensional AdS, and another one is a 5-sphere <sup>2</sup>. By bending some of the direction of space into compact manifolds it becomes possible to have a cosmological constant in supergravity theory, Because supergravity theories in the context of string theory, generally do not have a cosmological constant [1].

Consider an AdS in which a solid 4-dimensional spatial ball times the infinite time axis. The geometry is described by this metric:

$$d\tau^2 = \frac{R^2}{(1-r^2)^2} \{ (1+r^2)^2 dt^2 - 4dr^2 - 4r^2 d\Omega^2 \},$$
 (3.1)

where r is radial coordinate  $(0 \le r < 1)$ , t is time,  $\Omega$  is the unit

<sup>&</sup>lt;sup>2</sup>The main reason for the existence of the 5-dimensional is mathematical perception.

3-sphere, and R is the radius of curvature (geometry has uniform curvature  $R^{-2}$ ). The metric can be written in this form:

$$d\tau^2 = \frac{R^2}{y^2} \{ dt^2 - dx^i dx^i - dy^2 \}, \tag{3.2}$$

where i varies from 1 to 3.

The metric 3.2 is the exact metric of an incomplete patch of AdS space, and the metric has a horizon at  $y = \infty$ .

By change of coordinate  $(z = \frac{1}{y})$ , we can rewrite metric 3.2,

$$d\tau^2 = R^2 \left\{ z^2 (dt^2 - dx^i dx^i) - \frac{1}{Z^2} dz^2 \right\}.$$
 (3.3)

We can create  $AdS(5) \otimes S(5)$  by adding this term to the metric:

$$ds_5^2 = R^2 dw_5^2, (3.4)$$

where  $w_5$  is the metric of the unit 5-sphere.

#### 3.1.3 Holography in AdS space

Consider  $AdS(5) \otimes S(5)$  as the bulk space and the 4-dimensional boundary of AdS at y = 0 which is the boundary. Based on the Holographic principle, we can describe everything in the bulk by a theory on the boundary. But, the boundary theory has no more than 1 degree of freedom per plunk.

Metric 3.2 has a "dilatation" symmetry,

$$t \to \lambda t,$$
$$x^i \to \lambda x^i,$$
$$y \to \lambda y.$$

Plus, the full symmetry group of AdS(5) is the group O(4|2) and there is the symmetry O(6) associated with the rotation of the internal 5-sphere.

Because of the symmetry, a holographic boundary theory is invariant under the conformal group. On the other hand, the boundary has an infinite density of degree of freedom. Thus, **the holographic theory is a Conformal Quantum Field Theory**. The additional symmetry of space is the so-called  $\mathcal{N}=4$  supersymmetry. All of this leads us to the remarkable conclusion that quantum gravity in  $AdS(5) \otimes S(5)$  can be described by a superconformal Lorentz invariant quantum field theory associated with the AdS boundary [1].

### 3.2 Ads/CFT and Critical phenomena

Physics of critical phenomena describes a wide range of like phase transition, superconductivity, and some interesting issue in Condensed matter physics. One of the main purposes of this thesis is to take advantage of Ads/CFT to derive the scaling behavior of order parameters near a critical point of conductivity in a Weyl semimetal [36].

A couple of years after the publication of the famous paper of Maldacena [32], physicists discover some holographic models to describe some phenomena in the condensed matter and statistical physics <sup>3</sup>.

#### 3.2.1 Quantum phases

The classical solid, liquid and gaseous phases involve different configurations of atoms or molecules, governed by temperature [42]. By quantum mechanics, we can discover some quantum phases which are associated with statistical mechanics and some principles like the Pauli exclusion principle. These quantum phases are summarized in Figure 3.2 and Figure 3.3 which are adapted from Ref. [42].

Quantum Phases Metals conduct electricity readily. Their electrons hopscotch from atom to atom, and if the atoms provide enough sites for the electrons to occupy, the electrons move freely, as if in a gas. Quantum effects limit the number of electrons that can have a given amount of energy.

Insulators scarcely conduct electricity at all. The atoms do not provide enough vacancies for the itinerant electrons, so electrons remain trapped in place, as if in a solid. They occupy all the available energy slots.

Superconductors are gases not of electrons but of pairs of electrons that behave as single particles. The electrons pair up under the effects of quantum spin or the influence of waves rippling through the atomic substrate. These pairs evade

the quantum rules governing electrons. All of them can have the same amount of energy—lifting the restrictions that trap electrons in place and letting them flow without electrical resistance.

A spin-density wave (not shown) is a material (sometimes an insulator, sometimes a superconductor) with a peculiar pattern of electron spins. Half are spinning up, half down—say, in alternating rows. Sometimes a strange metal—a spin-density wave taken to extremes—forms [see phase diagram on opposite page]. The probability of each individual electron spinning up or down is 50-50, with no broader patterns. All the electrons in a strange metal are entangled and behave neither as individual particles nor even as pairs but as masses of trillions or more particles.

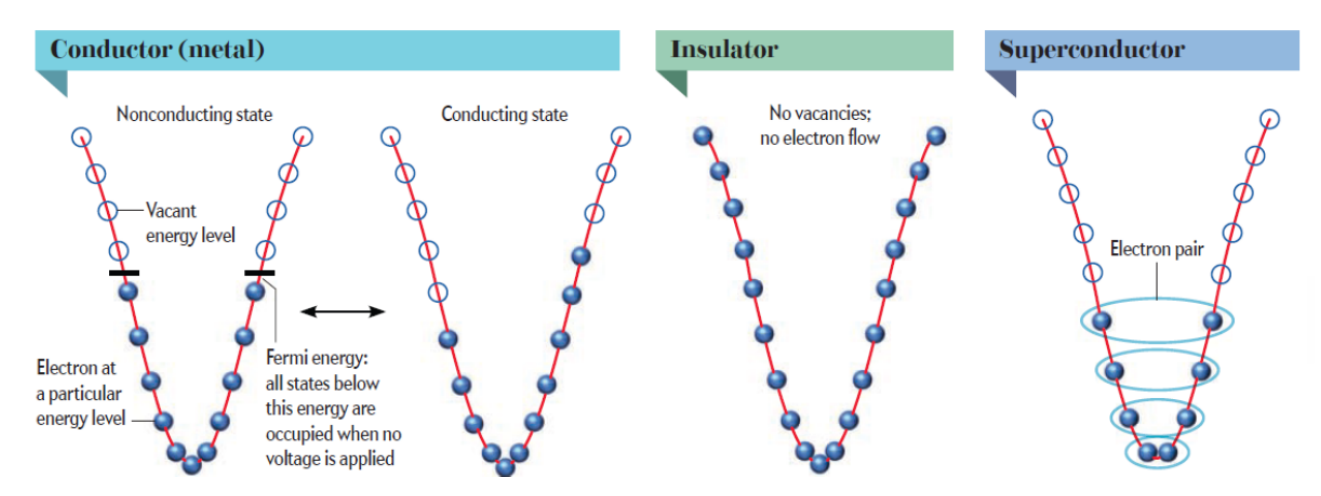


Figure 3.2: Quantum phases

<sup>&</sup>lt;sup>3</sup>See for instance [37], [38], [39], [40] and [41].

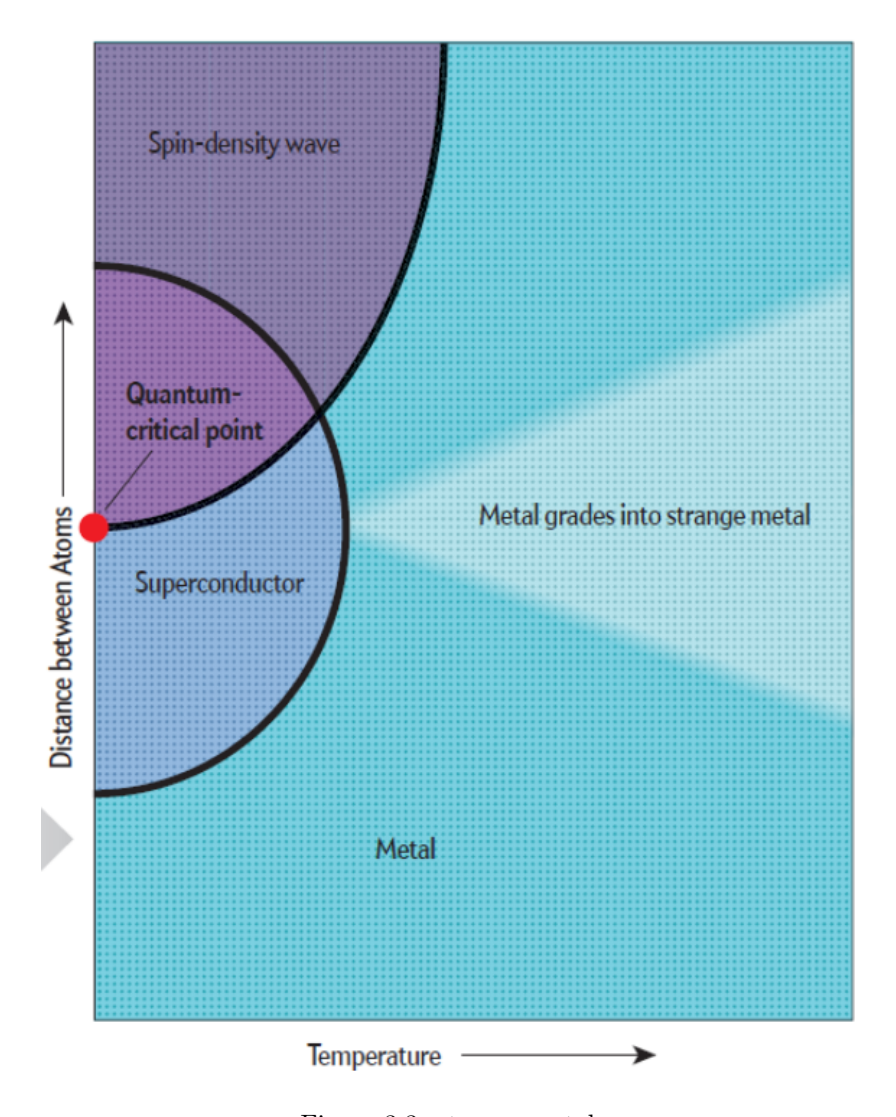


Figure 3.3: strange metal

#### 3.2.2 Holographic DC conductivities from the open string metric

As mentioned the AdS/CFT correspondence is a powerful tool for studying the dynamics of strongly coupled field theory. One of the important applications of AdS/CFT is to compute transport coefficients in the strongly coupled field theory such as various conductivities [43]. In this thesis, we focus on DC conductivity. In the context of condensed matter theory, conductivity is particularly interesting in the strange metal phases of heavy fermion compounds and high-temperature superconductors [43]. We are going to study the DC conductivity of charge carriers interacting with a strongly coupled gauge theory.

There are three holographic methods to compute the DC conductivity [43]:

- (1) the retarded Green's function method [44].
- (2) the membrane paradigm method [45].
- (3) the real-action method [37].

In this thesis, we going to take advantage of the real-action method.

#### 3.2.3 the real-action method

The real-action method is tailored for DC conductivity. It can be applied only to probe D-brane systems described by the DBI action (actually in this method we make the DBI action real). The real-action method yields a non-linear conductivity while methods (1) and (2) yield a linear conductivity [43].

## Chapter 4

# The Real-Action Method, Chiral Magnetic Effect, and Weyl Semimetal

In this chapter, we are going to review quickly Karch-O'Bannon's real-action method [37]. Then, using Real-Action Method we study the Chiral Magnetic Effect, and a Weyl semimetal in the context of AdS/CFT [46, 47].

#### 4.1 Karch-O'Bannon's real-action method

This section is a review of Ref.[37].

#### 4.1.1 Metallic AdS/CFT

To study the DC conductivity of charge carriers interacting with a strongly coupled gauge theory, we use a holographic model which is a probe brane system. In this model, the charge carriers are represented by a small number  $(N_f)$  of probe D-branes with a non-trivial temporal world volume gauge field (finite charge density). The strongly-coupled gauge field dynamics is encoded in a background geometry. By consider a large  $N_c(\gg N_f)$  gauge theory. In other words, we ignore the back-reactions of probe branes on the geometry.

Consider a linear (non-linear) conductivity which means an electric field independent (dependent) conductivity. For computing the conductivity we use Dirac-Born-Infield (DBI) for the probe brane. The DBI action of Dp-brane is

$$\int \xi^{p+1} \sqrt{\det(P[G] + F)},$$

where P[G] is the induced metric and F is the gauge field strength.

If the field E points in the x direction, say, we expect a constant, nonzero current  $\langle J^x \rangle$  and we can define a conductivity  $\sigma$  by

$$\langle J^x \rangle = \sigma E. \tag{4.1}$$

#### 4.1.2 The prob brane and conductivity

In this subsection, we going to compute conductivity. Note that we will focus on calculation (shut up and calculate!). Some technical issues and details can be found in Ref.[37] and [43].

We define the  $AdS_5$  metric in Lorentzian signature and in units where the radius of AdS is one,

$$ds^{2} = \frac{dz^{2}}{z^{2}} - \frac{1}{z^{2}} \frac{(1 - z^{4}/z_{H}^{4})^{2}}{1 + z^{4}/z_{H}^{4}} dt^{2} + \frac{1}{z^{2}} (1 + z^{4}/z_{H}^{4}) d\vec{x}^{2}, \tag{4.2}$$

where  $z_H^{-1} = \frac{1}{\sqrt{2}}T$  and  $d\vec{x}^2$  is the metric of three-dimensional Euclidean space. The  $S^5$  metric is

$$d\Omega_5^2 = d\theta^2 + \sin^2\theta d\psi^2 + \cos^2\theta d\Omega_3^2, \tag{4.3}$$

where  $d\Omega_3^2$  is the standard metric for an  $S^3$  and  $\theta$  runs from zero to  $\pi/2$ .

Now we are going to write down the DBI <sup>1</sup> for a number  $N_f$  of D7-branes filling  $AdS_5$  and wrapping the  $S^3 \subset S^5$ :

$$S_{D7} = -N_f T_{D7} \int d^8 \xi \sqrt{-\det(g_{ab} + (2\pi\alpha')F_{ab})}, \tag{4.4}$$

where  $T_{D7}$  is the D7-brane tension,  $\xi$  is its worldvolume coordinates,  $g_{ab}$  is the induced worldvolume metric and  $F_{ab}$  is the worldvolume U(1) field strength.

We take an embedding function  $\theta(z)$  to describe the position of the  $S^3$  on the  $S^5$  as well as worldvolume gauge fields  $A_t(z)$  and  $A_x(z,t)$ . Thus,

$$S_{D7} = -\mathcal{N} \int dz dt \cos^{3}\theta g_{xx}$$

$$\sqrt{|g_{tt}|g_{xx}g_{zz} - (2\pi\alpha')^{2} \left(g_{xx}A'_{t}(z)^{2} + g_{zz}\dot{A}_{x}(z,t)^{2} - |g_{tt}|A'_{x}(z,t)^{2}\right)},$$
(4.5)

<sup>&</sup>lt;sup>1</sup>We take Wess-Zumino term zero.

where  $g_{zz} = 1/z^2 + '(z)^2$ .

We take  $A_x(z,t) = -Et + h(z)$ . Thus, we have conserved charges. The conserved charge associated with  $A_t$  is

$$\cos^{3} g_{xx} \frac{-\mathcal{N}(2\pi\alpha')^{2} g_{xx} A_{t}'(z)}{\sqrt{|g_{tt}| g_{xx} g_{zz} - (2\pi\alpha')^{2} \left(g_{xx} A_{t}'(z)^{2} + g_{zz} \dot{A}_{x}(z,t)^{2} - |g_{tt}| A_{x}'(z,t)^{2}\right)}}} \equiv D_{xx} \frac{-\mathcal{N}(2\pi\alpha')^{2} g_{xx} A_{t}'(z)}{\sqrt{|g_{tt}| g_{xx} g_{zz} - (2\pi\alpha')^{2} \left(g_{xx} A_{t}'(z)^{2} + g_{zz} \dot{A}_{x}(z,t)^{2} - |g_{tt}| A_{x}'(z,t)^{2}\right)}}}$$
(4.6)

The second charge, associated with  $A_x(z,t)$ , is

$$\cos^{3} g_{xx} \frac{\mathcal{N}(2\pi\alpha')^{2} |g_{tt}| h'(z)}{\sqrt{|g_{tt}| g_{xx} g_{zz} - (2\pi\alpha')^{2} \left(g_{xx} A'_{t}(z)^{2} + g_{zz} \dot{A}_{x}(z,t)^{2} - |g_{tt}| A'_{x}(z,t)^{2}\right)}}} \equiv E_{t}(4.7)$$

Finally, by considering boundary conditions, we can find near the z=0 boundary the gauge fields asymptotically approach

$$A_t(z) = \mu - \frac{1}{2} \frac{D}{\mathcal{N}(2\pi\alpha')^2} z^2 + O(z^4), \tag{4.8}$$

$$h(z) = b + \frac{1}{2} \frac{B}{\mathcal{N}(2\pi\alpha')^2} z^2 + O(z^4). \tag{4.9}$$

One can show

$$\langle J^t \rangle = D, \qquad \langle J^x \rangle = B.$$
 (4.10)

We can write the action in terms of D, B, and E with one dynamical field  $\theta(z)$ ,

$$S_{D7} = -\mathcal{N} \int dz dt \cos^6 g_{xx}^{5/2} |g_{tt}|^{1/2} \sqrt{\frac{g_{zz}(|g_{tt}|g_{xx} - (2\pi\alpha')^2 E^2)}{|g_{tt}|g_{xx}^3 \cos^6 + \frac{|g_{tt}|D^2 - g_{xx}B^2}{\mathcal{N}^2(2\pi\alpha')^2}}}.$$
(4.11)

For making action in equation 4.11 real, at point  $z=z_*$  we must have:

$$|g_{tt}|g_{xx} - (2\pi\alpha')^2 E^2 = 0 (4.12)$$

$$|g_{tt}|g_{xx}^3\cos^6(z_*) + \frac{|g_{tt}|D^2 - g_{xx}B^2}{\mathcal{N}^2(2\pi\alpha')^2} = 0$$
 (4.13)

In the end, by using equations 4.12 and 4.13 we will find the conductivity:

$$\sigma = \sqrt{\frac{N_f^2 N_c^2 T^2}{16^2} \sqrt{e^2 + 1} \cos^6(z_*) + \frac{d^2}{e^2 + 1}},$$
 (4.14)

where

$$e = \frac{E}{\frac{\pi}{2}\sqrt{\lambda}T^2},$$
 
$$d = \frac{D}{\frac{\pi}{2}\sqrt{\lambda}T^2} = \frac{J^t}{\frac{\pi}{2}\sqrt{\lambda}T^2}.$$

### 4.2 Negative Differential Resistivity

Shin Nakamura found an interesting phase transition of current in the holographic model which we mention in the previous section [48]. In equation 4.11 the action has one dynamical field  $\theta(z)$ . Nakamura solves the equation of motion for  $\theta(z)$  numerically. The equation of motion is a second-order differential equation. He takes two initial conditions to solve this differential equation. First initial condition: for given E we compute  $z_*$ , then we assign  $0 < \theta(z_*) < \frac{\pi}{2}$  and compute J. Second initial condition:  $\theta'(z_*)$  can be found by expanding  $\theta(z_*)$  around  $z_*$ .

The transition occurs when the sign of the differential conductivity reverses. More details can be found in Ref. [48], also this method examines by turning on a magnetic field in different backgrounds [49], [50].

## 4.3 Chiral Magnetic Effect

# 4.3.1 Reviewing of Chiral Magnetic effect from Probe branes holography

The probe branes holography is constructed from  $N_f$  flavor branes as a probe in the background of  $N_c$  color branes. In the duality to the supergravity limit of this system, the  $N_f$  branes consider as a fundamental matter and  $N_c$  branes as a background gauge theory.

Considering D7 branes as probes in D3 branes we have a supersymmetric QCD-like system as a dual-field theory (see [51] and references therein).

In the limit  $N_c \to \infty$  and for the large 't Hooft coupling, the background D3-branes are replaced by the extremal supergravity solution

which is  $AdS_5 \times S^5$ . This system is dual to  $\mathcal{N} = 4$  super Yang-Mills theory( $SU(N_c)$ ) in 1 + 3 dimension. The near extremal solution of the D3 brane would be a Schwartzshild-AdS space-time which is dual to the quantum system at non-zero temperature <sup>2</sup>, in the unit of AdS radius, we choose it with the following coordinates

$$ds^{2} = -|g_{tt}|dt^{2} + g_{xx}d\vec{x}^{2} + g_{rr}dr^{2} + g_{\theta\theta}d\theta^{2} + g_{\phi\phi}d\phi^{2} + g_{SS}d\Omega_{3}^{2}, (4.15)$$

where

$$g_{tt} = \frac{1}{r^2} f(r), \quad g_{xx} = \frac{1}{r^2}, \quad g_{rr} = \frac{1}{r^2} f^{-1}(r),$$

$$g_{\theta\theta} = 1, \quad g_{\phi\phi} = \sin^2 \theta, \quad g_{SS} = \cos^2 \theta.$$
(4.16)

In the above,  $f(r) = (1 - r^4/r_h^4)$  and  $d\Omega_3^2$  is the metric of a unit 3-sphere( $S^3$ ). In this choice of coordinates, the boundary of the AdS is located at  $r \to 0$  and the field theory lives in 1+3 dimension Minkowski space with coordinates  $(t, \vec{x})$ . The  $r_h$  indicates the location of the horizon of the black hole and is related to the Hawking temperature, which is also the temperature of our state in the dual field theory, by

$$T = \frac{1}{\pi r_b}.\tag{4.17}$$

Eq(4.15) will change to  $AdS_5 \times S^5$ . In this background, we also have a self-dual R-R five form field  $F_5 = dC_4$  where

$$C_4 = g_{xx}^2 \operatorname{vol}_{R^{1,3}} - g_{SS}^2 d\phi \wedge \operatorname{vol}_{S^3}. \tag{4.18}$$

Consider the intersection of  $N_c$  stack of D3-branes and  $N_f$  stack of the D7-branes which embedded in ten dimension space-time as Table (4.1),

	t	$\vec{x}$	r	$S^3$	$\theta$	$\phi$
D3	×	×	×			
D7	×	×	×	×		

Table 4.1: D3 - D7 embedding.

The probe limit elaborate with  $\frac{N_f}{N_c} \ll 1$  with this assumption the dynamics of probe D7-branes is given by the addition of DBI action and Wess-Zumio term

$$S_{D7} = S_{DBI} + S_{WZ}, (4.19)$$

 $<sup>^{2}</sup>$ At non-zero temperature fermions and bosons obey different statistics, so in this case, the supersymmetry is broken explicitly.

$$S_{DBI} = -N_f T_{D7} \int d^8 \sigma \sqrt{-\det(P[g_{ab}] + (2\pi\alpha') F_{ab})},$$
 (4.20)

$$S_{WZ} = +\frac{1}{2} N_f T_{D7} (2\pi\alpha')^2 \int P[C_4] \wedge F \wedge F, \qquad (4.21)$$

where  $T_{D7} = \frac{g_s^{-1}}{(2\pi)^7}$  is the D7-brane tension,  $\sigma^a$  is the world volume coordinates,  $P[g_{ab}]$  is the induced metric on the probe branes or pullback of the background metric to the D7-branes,  $F_{ab}$  is the U(1) worldvolume field strength, and  $P[C_4]$  is the pullback of the RR fourform to the probe D7-branes.

With the embedding as table(4.1), where the probe D7-branes extended along  $AdS_5 \times S^3$ , there is a rotational symmetry in  $(\theta, \phi)$ -plane which resembles a global axial  $U_A(1)$  symmetry. We could break the rotational symmetry by considering  $\theta = \theta(r)$ . We could relate those assumptions to the flavor fermionic (quark) sector mass in the dual theory. We could also simulate the chiral anomaly in the dual field theory by attributing the angular velocity  $\omega$  to the probe branes by considering  $\phi(t,r) = \omega t + \varphi(r)^3$ . But considering rotating probe branes with constant angular velocity  $\omega$  the flavor fermion mass would be a complex quantity  $|m| e^{i\phi(t,r)}$  [47, 52]. It is shown that in [47] the time-dependent part of the phase of the complex mass or probe brane angular velocity leads to the chiral anomaly in the dual field theory. As pointed out in [47] the angular velocity  $\omega$  is a bulk dual of axial chemical potential  $\mu_5$  in the boundary QFT [47],

$$\omega = 2\mu_5. \tag{4.22}$$

To study the chiral magnetic effect we introduce a constant magnetic field B on the probe D7-branes. Also to find out the system's response to doing this external field we assume the U(1) gauge field on the D7-brane as follows,

$$2\pi\alpha' F_{xy} = B, \quad 2\pi\alpha' F_{rz} = \partial_r A_z(r)^4. \tag{4.23}$$

With these assumptions, we can rewrite  $S_{D7}$ . The real condition of the action coincides with the world-volume horizon of the probe

<sup>&</sup>lt;sup>3</sup>The second term,  $\varphi(r)$ , is for avoiding tachyonic instability or in other words the non-zero  $\varphi(r)$  is for avoiding the linear velocity of rotating probe branes to exceed the local speed of light, for more details see [47].

<sup>4</sup>Note that we consider  $\vec{x} = (x, y, z)$ .

D7 brane. Following [47] the world-volume horizon  $r_*$  is given by the following equations

$$|g_{tt}(r_*)| - g_{\phi\phi}(r_*)\omega^2 = 0$$
 (4.24a)

$$\mathcal{N}^2 (1 + \frac{B^2}{g_{xx}^2}) |g_{tt}| g_{\phi\phi} g_{xx}^3 g_{SS}^3 |_{r_*} = \alpha^2$$
 (4.24b)

$$-\mathcal{N}B\omega g_{SS}^2(r_*) = \beta \tag{4.24c}$$

From the near boundary solution and AdS/CFT correspondence, we would know that [20],

$$\langle J^z \rangle = -2\pi \alpha' \beta \tag{4.25}$$

therefore we could observe the chiral magnetic effect

$$\langle J^z \rangle = \sigma^{\chi} \tilde{B}, \tag{4.26}$$

where from Eq.(4.23) we recover the magnetic field  $\tilde{B}$  of boundary QFT by  $2\pi\alpha'\tilde{B}=B$  and we define  $\sigma^{\chi}=(2\pi\alpha')^2\mathcal{N}\omega g_{SS}^2(r_*)$  as the chiral magnetic conductivity(CMC).

The non-zero current means that the magnetic field will turn apart strings with both ends located on a probe rotating branes similar to the electric field on the static branes [37]. Therefore the current  $\langle J^z \rangle$  will be produced<sup>5</sup>. For the mass-less flavor, we have  $g_{SS} = 1$  so the CMC is determined by chemical axial potential,

$$\sigma^{\chi} = \frac{N_f N_c}{2\pi^2} \mu_5.6 \tag{4.27}$$

We could intemperate the  $r_*$  as a location of the world-volume horizon which obviously is different from the background horizon. Hence, we are able to assign an effective temperature in the dual boundary theory to it, see [54, 55]. It is clear from Eq(4.24a) that for zero angular velocity  $\omega$  we have  $r_* = r_h$  even at the non-zero magnetic field, see also [52]. In the dual field theory, this statement means that if we do not have chiral asymmetry between left-handed and right-handed flavors or zero axial chemical potential  $\mu_5$  the magnetic field will not generate CME. So for the non-zero  $\omega$ , we should deal with other classes of probe brane embedding which differs from the ME and BE. We call it Minkowski embedding with (world-volume) horizon(MEH). This is

The amplitude of pair production from  $\langle J^z \rangle = 0$  to  $\langle J^z \rangle \neq 0$  due to the external magnetic field in this situation studied in [53].

<sup>&</sup>lt;sup>6</sup>Note that we use  $(2\pi\alpha')^2 = \frac{2\pi}{\lambda}$ .

similar to the non-rotating probe branes in the presents of an external electric field in which we have a non-zero current for the BH and MEH embedding. To clarify this statement we do the same numerical analysis as [48, 49, 50, 56] by solving the following equation

$$\frac{\partial \mathcal{L}}{\partial \theta} - \frac{d}{dr} \left( \frac{\partial \mathcal{L}}{\partial \theta'} \right) = 0, \tag{4.28}$$

with two boundary condition on the location of world-volume horizon  $r_*$ , i.e,  $\theta(r_*)$  and  $\theta'(r_*)$ . Among the interval  $0 < \theta(r_*) < \pi/2$ , we select a value for  $\theta(r_*)$ . The other condition,  $\theta'(r_*)$ , obtain by inserting linear order expansion of  $\theta(r)$  near  $r_*$  .i.e.,

$$\theta(r) = \theta(r_*) + (r - r_*)\theta'(r_*) + \dots \tag{4.29}$$

to the Eq.(4.28). With these two initial or boundary conditions, we solve numerically Eq.(4.28) and from the  $2\pi\alpha'm = \lim_{r\to 0} \frac{\theta(r)}{r}$  we read the mass m of the fermion flavors. For the fixed value of magnetic field B and also fixed background temperature T and angular velocity  $\omega$ , for a specific value for current  $J^z$  we could correspond a flavor's mass. Finally, we will find the mass-current relation through figure 4.2

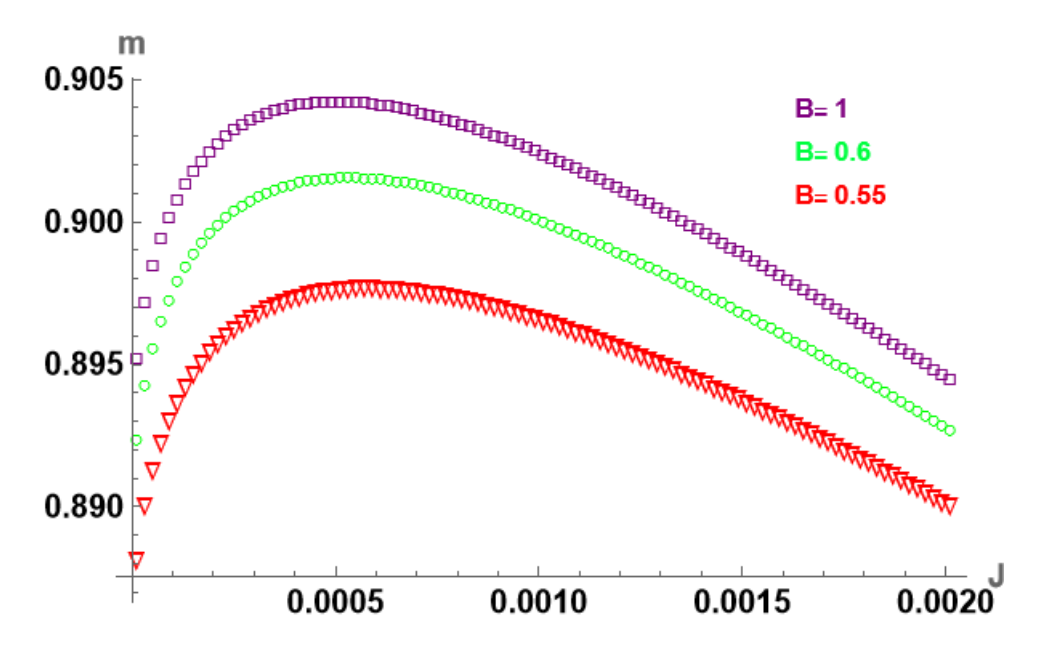


Figure 4.1:  $m_q$ -J curve for different values of B at T=0.31878 and  $\mu_5=0.05$ . The maximum values are located at  $m_{max}=0.904,\,0.901,\,$  and 0.898; from top to bottom respectively.

It is clear that for small current regions, we have two currents with the same mass. This is a signature of the existence of both solutions, MEH and BE. As it is evident in the figure, there is a maximum mass where for the criteria  $m > m_{max}$  there is no current so we interpret that region as a Minkowski embedding(ME)<sup>7</sup>. Non-zero current

<sup>&</sup>lt;sup>7</sup>So we have numerical insight about the magnitude of  $\frac{m}{T}$  ratio which is discussed before.

as mentioned means that the string with both ends on the same brane will tear apart which in the dual theory means the bound between fermion anti-fermion will break and the system will transit from ME J=0 to MEH or BH with  $J\neq 0$ . We call the state with non-zero current a conducting phase and the zero current state an insulator state or phase. Or confinement and deconfinement state respectively. Having two embedding with non-zero currents or two conducting states same as metallic AdS/CFT [48, 49, 56]. So, we will continue the next section to study numerically the CMC for a massive flavor sector.

#### 4.3.2 Results and discussion

As already observed we have two different currents for a fixed mass in the previous section. So it would be interesting if we fix mass and explore the behavior of chiral magnetic conductivity by illustrating the (J-B)'s plot. Unlike the previous cases of studied phase transitions in the gravity duality, for this chiral magnetic conductivity, we do not see a phase transition occurring via the parameter  $u_h$ , which is related to the Hawking temperature Eq.(4.17). The only active parameter for a phase transition is the  $\omega$ .

In figure (2), we see a phase transition occurring for our Chiral magnetic differential current, with respect to the external field parameter of B, and  $\omega$ . We also see a second-order continuous phase transition at  $\omega = 1.4$ , changing to a first-order non-continuous transition, with the critical value of  $\omega_c = 1.2$  in between. It is noteworthy to mention that the J-B diagram will have a multi-valued behavior, at some region of B for the first-order transitions of  $\omega < \omega_c$ . In a physical system, only the points with the lowest energy are expected to be occurring in the system. This condition will determine the exact point of the discontinuous transition, which will become handy in the determination of the critical exponents. In the case of metallic AdS/CFT [48, 49, 56, 57]. the study of electric conductivity reveals the negative differential conductivity(NDC) to positive differential conductivity (PDC) phase transition. For the chiral conductivity as is clear from figure (2), by changing the axial chemical potential the structure of phases will change but we have NDC to NDC phase transition.

Also, We explore other phase transitions. One is a phase transition which is shown in figure 4.3  $\mu_5 - J$  for different Values of B. Other phase transitions and the critical exponents can be found in Ref[58].

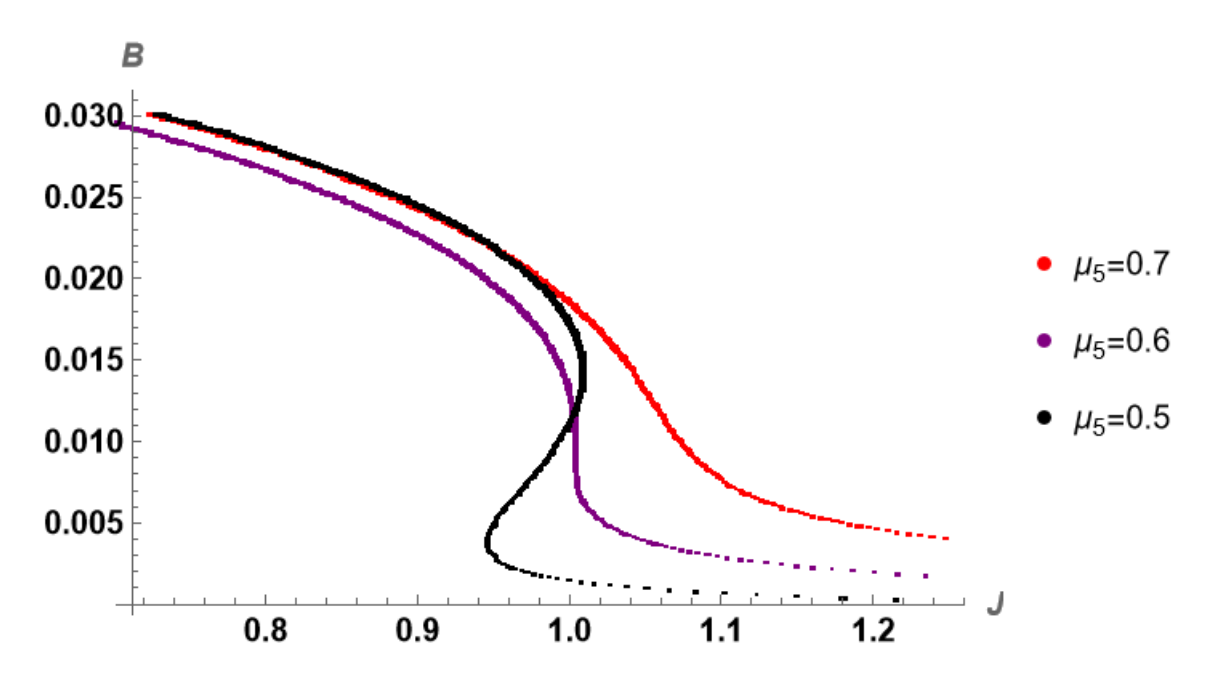


Figure 4.2: B-J curve for different values of  $\mu_5$  at T=0.31878 and m=0.902. The Calculated value of  $\mu_{5c}=0.597$ .

# 4.4 Negative Differential Resistivity of a Weyl Semimetal from AdS/CFT

In the last stage of this thesis, we study the phase transition of current in the holographic model of a Weyl Semimetal. This holographic model is mentioned in Ref. [46].

In this holographic model, the metric and the four-form, C4 are given by

$$ds^{2} = \frac{\rho^{2}}{L^{2}} \left(-\frac{g^{2}(\rho)}{h(\rho)}dt^{2} + h(\rho)d\vec{x}^{2}\right) + \frac{L^{2}}{\rho^{2}}(dr^{2} + r^{2}ds_{S^{3}}^{2} + dR^{2} + R^{2}d\phi^{2}),$$
(4.30)

$$C_4 = \frac{\rho^4}{L^4} h^2(\rho) dt \wedge dx \wedge dy \wedge dz - \frac{L^4 r^4}{\rho^4} d\phi \wedge \omega(S^3), \tag{4.31}$$

where  $\rho^2 = r^2 + R^2$ ,  $g(\rho) \equiv 1 - \frac{\rho_H^4}{\rho^4}$ , and  $h(\rho) \equiv 1 + \frac{\rho_H^4}{\rho^4}$ .

Based on Ref. [46], in this background, we can write DBI action in the following form:

$$\tilde{S}_{D7} = -\mathcal{N} \int dr \sqrt{h} \sqrt{1 + R'^2} \sqrt{\alpha(r)\beta(r) - \gamma(r)}, \qquad (4.32)$$

where

$$\alpha(r) \equiv g^2 - \frac{L^4 E^2}{(r^2 + R^2)^2}$$

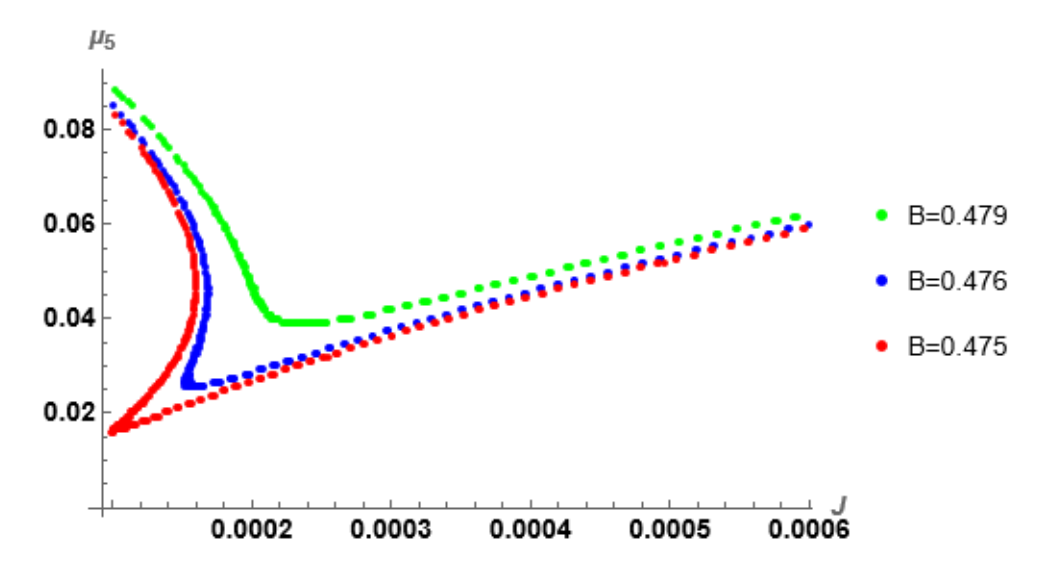


Figure 4.3: J- $\omega$  curve at T = 0.31878 and m = 0.902.

$$\beta(r) \equiv r^6 \left(h + \frac{L^4 b^2 R^2}{\left(r^2 + R^2\right)^2}\right) - \frac{j_x^2}{g^2}$$

$$\gamma(r) \equiv \frac{p_\phi^2}{h^2} \left(\frac{h}{R^2} + \frac{L^4 b^2}{\left(r^2 + R^2\right)^2}\right) + \left(j_y - \frac{L^4 r^4 b E}{\left(r^2 + R^2\right)^2}\right)^2.$$

The action (4.32) has one dynamical field R(r). Thus, we can solve the equation of motion for R(r) based on the Nakamura method which we mentioned. The numerical methods and the result will publish in Ref. [36] which is in progress.

# Appendix A General relativity

# $\begin{tabular}{ll} Appendix A \\ Strings and D-branes \\ \end{tabular}$

## **Bibliography**

- [1] L. Susskind and J. Lindesay. An introduction to black holes, information and the string theory revolution: The holographic universe. 2005.
- [2] Walter Greiner; Ludwig Neise; Horst Stöcker. The Thermodynamics and statistical mechanics Book. New York: Springer-Verlag, 1995.
- [3] Lisa Dyson, Matthew Kleban, and Leonard Susskind. "Disturbing implications of a cosmological constant". In: *JHEP* 10 (2002), p. 011. DOI: 10.1088/1126-6708/2002/10/011. arXiv: hep-th/0208013.
- [4] Aurel Wintne. The Analytical Foundations of Celestial Mechanics Book. Oxford University Press, 1947.
- [5] P.Bocchieri and A.Loinger. "Quantum recurrence theorem". In: Phys.Rev 107.337 (1957).
- [6] Stephen J. Blundell and Katherine M. Blundell.r. *Concepts in thermal physics Book*. Oxford ; Oxford University Press, 2010.
- [7] J. Preskill. Lecture Notes on Quantum Computation. http://www.theory.caltech.edu/people/preskill/ph229/, 1998.
- [8] Claude Elwood Shannon. "A mathematical theory of communication". In: Bell Syst. Tech. J. 27 (1948), pp. 379–423.
- [9] Stephen M Barnett. Quantum information Book. Oxford: Oxford University Press., 2012.
- [10] Tom Lancaster and Stephen J. Blundell. Quantum Field Theory for the Gifted Amateur. Oxford University Press, 2014. ISBN: 978-0-19-969933-9.
- [11] M. P. Hobson, G. P. Efstathiou, and A. N. Lasenby. General relativity: An introduction for physicists. 2006.
- [12] Bernard F. Schutz. A FIRST COURSE IN GENERAL RELATIVITY. Cambridge, UK: Cambridge Univ. Pr., 1985.
- [13] Robert M. Wald. General Relativity. Chicago, USA: Chicago Univ. Pr., 1984. DOI: 10.7208/ chicago/9780226870373.001.0001.
- [14] Klaas Landsman. "Penrose's 1965 singularity theorem: From geodesic incompleteness to cosmic censorship". In: (May 2022). arXiv: 2205.01680 [physics.hist-ph].
- [15] Klaas Landsman. "Singularities, black holes, and cosmic censorship: A tribute to Roger Penrose". In: Found. Phys. 51.2 (2021), p. 42. DOI: 10.1007/s10701-021-00432-1. arXiv: 2101.02687 [gr-qc].
- [16] Juan Maldacena and Leonard Susskind. "Cool horizons for entangled black holes". In: Fortsch. Phys. 61 (2013), pp. 781–811. DOI: 10.1002/prop.201300020. arXiv: 1306.0533 [hep-th].
- [17] Jerry B. Marion Stephen T. Thornton. The Classical Dynamics of Particles and Systems Book. Brooks/Coles, 2005, 5th Edition.
- [18] Raphael Bousso. "The Holographic principle". In: Rev. Mod. Phys. 74 (2002), pp. 825–874.
  DOI: 10.1103/RevModPhys.74.825. arXiv: hep-th/0203101.
- [19] Amanda W. Peet. "TASI lectures on black holes in string theory". In: Theoretical Advanced Study Institute in Elementary Particle Physics (TASI 99): Strings, Branes, and Gravity. Aug. 2000, pp. 353-433. DOI: 10.1142/9789812799630\_0003. arXiv: hep-th/0008241.
- [20] Leonard Susskind. "Black Hole-String Correspondence". In: (Oct. 2021). arXiv: 2110.12617 [hep-th].

BIBLIOGRAPHY BIBLIOGRAPHY

[21] Yiming Chen, Juan Maldacena, and Edward Witten. "On the black hole/string transition". In: (Sept. 2021). arXiv: 2109.08563 [hep-th].

- [22] B. Zwiebach. A first course in string theory. Cambridge University Press, July 2006. ISBN: 978-0-521-83143-7, 978-0-511-20757-0.
- [23] S. W. Hawking. "Breakdown of Predictability in Gravitational Collapse". In: *Phys. Rev. D* 14 (1976), pp. 2460–2473. DOI: 10.1103/PhysRevD.14.2460.
- [24] Ahmed Almheiri et al. "The entropy of Hawking radiation". In: Rev. Mod. Phys. 93.3 (2021), p. 035002. DOI: 10.1103/RevModPhys.93.035002. arXiv: 2006.06872 [hep-th].
- [25] Gerard 't Hooft. "Dimensional reduction in quantum gravity". In: Conf. Proc. C 930308 (1993), pp. 284–296. arXiv: gr-qc/9310026.
- [26] Leonard Susskind. "The World as a hologram". In: J. Math. Phys. 36 (1995), pp. 6377–6396.
   DOI: 10.1063/1.531249. arXiv: hep-th/9409089.
- [27] Ofer Aharony et al. "Large N field theories, string theory and gravity". In: *Phys. Rept.* 323 (2000), pp. 183–386. DOI: 10.1016/S0370-1573(99)00083-6. arXiv: hep-th/9905111.
- [28] Johanna Erdmenger. "Introduction to Gauge/Gravity Duality". In: PoS TASI2017 (2018), p. 001. DOI: 10.22323/1.305.0001. arXiv: 1807.09872 [hep-th].
- [29] Horatiu Nastase. Introduction to the ADS/CFT Correspondence. Cambridge University Press, Sept. 2015. ISBN: 978-1-107-08585-5, 978-1-316-35530-5.
- [30] Henry W. Lin et al. "Holography for people with no time". In: (July 2022). arXiv: 2207.00407 [hep-th].
- [31] Makoto Natsuume. AdS/CFT Duality User Guide. Vol. 903. 2015. ISBN: 978-4-431-55441-7, 978-4-431-55440-0. DOI: 10.1007/978-4-431-55441-7. arXiv: 1409.3575 [hep-th].
- [32] Juan Martin Maldacena. "The Large N limit of superconformal field theories and supergravity". In: Adv. Theor. Math. Phys. 2 (1998), pp. 231–252. DOI: 10.1023/A:1026654312961. arXiv: hep-th/9711200.
- [33] David McMahon. The String Theory Demystified Book. McGraw-Hill Professional, 2008, 1th Edition.
- [34] Leonard Susskind and Edward Witten. "The Holographic bound in anti-de Sitter space". In: (May 1998). arXiv: hep-th/9805114.
- [35] Edward Witten. "Anti-de Sitter space and holography". In: Adv. Theor. Math. Phys. 2 (1998), pp. 253–291. DOI: 10.4310/ATMP.1998.v2.n2.a2. arXiv: hep-th/9802150.
- [36] A. Vahedi A. Hosseinzadeh. Negative Differential Resistivity of a Weyl Semimetal from AdS/CFT. in progress.
- [37] Andreas Karch and Andy O'Bannon. "Metallic AdS/CFT". In: *JHEP* 09 (2007), p. 024. DOI: 10.1088/1126-6708/2007/09/024. arXiv: 0705.3870 [hep-th].
- [38] Subir Sachdev. "What can gauge-gravity duality teach us about condensed matter physics?" In: Ann. Rev. Condensed Matter Phys. 3 (2012), pp. 9-33. DOI: 10.1146/annurev-conmatphys-020911-125141. arXiv: 1108.1197 [cond-mat.str-el].
- [39] Nabil Iqbal, Hong Liu, and Mark Mezei. "Lectures on holographic non-Fermi liquids and quantum phase transitions". In: *Theoretical Advanced Study Institute in Elementary Particle Physics: String theory and its Applications: From meV to the Planck Scale.* Oct. 2011, pp. 707–816. DOI: 10.1142/9789814350525\_0013. arXiv: 1110.3814 [hep-th].
- [40] Sean A. Hartnoll. "Lectures on holographic methods for condensed matter physics". In: Class. Quant. Grav. 26 (2009). Ed. by A. M. Uranga, p. 224002. DOI: 10.1088/0264-9381/26/22/224002. arXiv: 0903.3246 [hep-th].
- [41] Subir Sachdev. "Statistical mechanics of strange metals and black holes". In: (May 2022). arXiv: 2205.02285 [hep-th].
- [42] Subir Sachdev. Strange and stringy. Scientific American. 308 (44): 44–51, 2013.
- [43] Keun-Young Kim and Da-Wei Pang. "Holographic DC conductivities from the open string metric". In: *JHEP* 09 (2011), p. 051. DOI: 10.1007/JHEP09(2011)051. arXiv: 1108.3791 [hep-th].

BIBLIOGRAPHY BIBLIOGRAPHY

[44] Dam T. Son and Andrei O. Starinets. "Minkowski space correlators in AdS / CFT correspondence: Recipe and applications". In: JHEP 09 (2002), p. 042. DOI: 10.1088/1126-6708/2002/09/042. arXiv: hep-th/0205051.

- [45] Pavel Kovtun, Dam T. Son, and Andrei O. Starinets. "Holography and hydrodynamics: Diffusion on stretched horizons". In: *JHEP* 10 (2003), p. 064. DOI: 10.1088/1126-6708/2003/10/064. arXiv: hep-th/0309213.
- [46] Kazem Bitaghsir Fadafan et al. "A Weyl semimetal from AdS/CFT with flavour". In: *JHEP* 04 (2021), p. 162. DOI: 10.1007/JHEP04(2021)162. arXiv: 2012.11434 [hep-th].
- [47] Carlos Hoyos, Tatsuma Nishioka, and Andy O'Bannon. "A Chiral Magnetic Effect from AdS/CFT with Flavor". In: *JHEP* 10 (2011), p. 084. DOI: 10.1007/JHEP10(2011)084. arXiv: 1106.4030 [hep-th].
- [48] Shin Nakamura. "Negative Differential Resistivity from Holography". In: *Prog. Theor. Phys.* 124 (2010), pp. 1105–1114. DOI: 10.1143/PTP.124.1105. arXiv: 1006.4105 [hep-th].
- [49] Mohammad Ali-Akbari and Ali Vahedi. "Non-equilibrium Phase Transition from AdS/CFT". In: Nucl. Phys. B 877 (2013), pp. 95–106. DOI: 10.1016/j.nuclphysb.2013.09.008. arXiv: 1305.3713 [hep-th].
- [50] Ali Vahedi and Mobin Shakeri. "Non-Equilibrium Critical Phenomena From Probe Brane Holography in Schrödinger Spacetime". In: *JHEP* 01 (2019), p. 047. DOI: 10.1007/JHEP01(2019) 047. arXiv: 1811.05823 [hep-th].
- [51] Steven S. Gubser and Andreas Karch. "From gauge-string duality to strong interactions: A Pedestrian's Guide". In: *Ann. Rev. Nucl. Part. Sci.* 59 (2009), pp. 145–168. DOI: 10.1146/annurev.nucl.010909.083602. arXiv: 0901.0935 [hep-th].
- [52] Sumit R. Das, Tatsuma Nishioka, and Tadashi Takayanagi. "Probe Branes, Time-dependent Couplings and Thermalization in AdS/CFT". In: *JHEP* 07 (2010), p. 071. DOI: 10.1007/JHEP07(2010)071. arXiv: 1005.3348 [hep-th].
- [53] Seyed Farid Taghavi and Ali Vahedi. "Equilibrium Instability of Chiral Mesons in External Electromagnetic Field via AdS/CFT". In: *JHEP* 06 (2016), p. 053. DOI: 10.1007/JHEP06(2016)053. arXiv: 1603.09264 [hep-th].
- [54] Arnab Kundu. "Effective Temperature in Steady-state Dynamics from Holography". In: *JHEP* 09 (2015), p. 042. DOI: 10.1007/JHEP09(2015)042. arXiv: 1507.00818 [hep-th].
- [55] Koji Hashimoto and Takashi Oka. "Vacuum Instability in Electric Fields via AdS/CFT: Euler-Heisenberg Lagrangian and Planckian Thermalization". In: *JHEP* 10 (2013), p. 116. DOI: 10.1007/JHEP10(2013)116. arXiv: 1307.7423 [hep-th].
- [56] Shin Nakamura. "Nonequilibrium Phase Transitions and Nonequilibrium Critical Point from AdS/CFT". In: *Phys. Rev. Lett.* 109 (2012), p. 120602. DOI: 10.1103/PhysRevLett.109. 120602. arXiv: 1204.1971 [hep-th].
- [57] Masataka Matsumoto and Shin Nakamura. "Critical Exponents of Nonequilibrium Phase Transitions in AdS/CFT Correspondence". In: Phys. Rev. D 98.10 (2018), p. 106027. DOI: 10.1103/PhysRevD.98.106027. arXiv: 1804.10124 [hep-th].
- [58] Navid Kazemi A.Hosseinzadeh A.Vahedi. *Holographic Chiral Magnetic effect and Non- Equilibrium Critical Phenomena*. to appear soon.